

JGR Atmospheres



RESEARCH ARTICLE

10.1029/2023JD039543

Special Section:

Southern Ocean clouds, aerosols, precipitation and radiation

Key Points:

- First vertically resolved measurements of ice nucleating particles (INPs) over the Southern Ocean, including in-cloud observations
- Correlation between normalized INP concentrations and wind speed suggests marine active site density is variable
- Higher ice nucleation efficiency observed above cloud, consistent with an increasing influence of mineral dust with height

Supporting Information:

Supporting Information may be found in the online version of this article.

Correspondence to:

K. A. Moore, kathryn.a.moore@colostate.edu

Citation:

Moore, K. A., Hill, T. C. J., McCluskey, C. S., Twohy, C. H., Rainwater, B., Toohey, D. W., et al. (2024). Characterizing ice nucleating particles over the Southern Ocean using simultaneous aircraft and ship observations. *Journal of Geophysical Research: Atmospheres*, 129, e2023JD039543. https://doi. org/10.1029/2023JD039543

Received 26 JUN 2023 Accepted 2 DEC 2023

Author Contributions:

Conceptualization: Kathryn A. Moore, Thomas C. J. Hill, Sonia M. Kreidenweis, Paul J. DeMott Data curation: Kathryn A. Moore

© 2024 The Authors.

This is an open access article under the terms of the Creative Commons Attribution-NonCommercial License, which permits use, distribution and reproduction in any medium, provided the original work is properly cited and is not used for commercial purposes.

Characterizing Ice Nucleating Particles Over the Southern Ocean Using Simultaneous Aircraft and Ship Observations

Kathryn A. Moore¹, Thomas C. J. Hill¹, Christina S. McCluskey², Cynthia H. Twohy^{3,4}, Bryan Rainwater^{5,6}, Darin W. Toohey⁵, Kevin J. Sanchez⁷, Sonia M. Kreidenweis¹, and Paul J. DeMott¹

¹Department of Atmospheric Science, Colorado State University, Fort Collins, CO, USA, ²Climate Global Dynamics Laboratory, NCAR, Boulder, CO, USA, ³NorthWest Research Associates, Redmond, WA, USA, ⁴Scripps Institution of Oceanography, University of California, San Diego, CA, USA, ⁵Department of Atmospheric and Oceanic Sciences, University of Colorado, Boulder, CO, USA, ⁶Now at Handix Scientific Inc., Fort Collins, CO, USA, ⁷NASA Langley Research Center, Hampton, VA, USA

Abstract Supercooled liquid clouds are ubiquitous over the Southern Ocean (SO), even to temperatures below -20°C, and comprise a large fraction of the marine boundary layer (MBL) clouds. Earth system models and reanalysis products have struggled to reproduce the observed cloud phase distribution and occurrence of cloud ice in the region. Recent simulations found the microphysical representation of ice nucleation and growth has a large impact on these properties, however, measurements of SO ice nucleating particles (INPs) to validate simulations are sparse. This study presents measurements of INPs from simultaneous aircraft and ship campaigns conducted over the SO in austral summer 2018, which include the first in situ observations in and above cloud in the region. Our results confirm recent observations that INP concentrations are uniformly lower than measurements made in the late 1960s. While INP concentrations below and above cloud are similar, higher ice nucleation efficiency above cloud supports model simulations that the dominant INP composition varies with height. Model parameterizations based solely on aerosol properties capture the mean relationship between INP concentration and temperature but not the observed variability, which is likely related to the only modest correlations observed between INPs and environmental or aerosol metrics. Including wind speed in addition to activation temperature in a marine INP parameterization reduces bias but does not explain the large range of observed INP concentrations. Direct and indirect inference of marine INP size suggests MBL INPs, at least during Austral summer, are dominated by particles with diameters smaller than 500 nm.

Plain Language Summary Although Antarctica is remote, the continent and the Southern Ocean (SO) that surrounds it play a fundamental role in shaping regional and global climate. The clouds in this region are unique, with less ice and more liquid water present at low temperatures than in other areas. This is likely related to very low concentrations of rare aerosol particles called ice nucleating particles (INPs), which cause liquid water droplets in clouds to freeze. Largely due to a lack of observations, SO clouds are poorly represented in global models, and the interactions between aerosol particles and clouds are one of the largest remaining uncertainties. This study presents results of INP measurements from several recent field campaigns over the SO, including the first observations within and above clouds in the region. Our results suggest different types of particles are present below and above clouds, which have varying ability to nucleate ice. They also highlight the need for additional measurements of INP composition and size, which are key variables needed to improve model simulations.

1. Introduction

The Southern Ocean (SO) surrounding Antarctica is frequently covered by vast tracts of low-level clouds, which have emerged as a key component in simulating regional and global climate, particularly the regional radiative budget (e.g., Bodas-Salcedo et al., 2013, 2016; Frey & Kay, 2017; Gettelman et al., 2020; Tan et al., 2016). Satellite retrievals suggest a greater occurrence of mixed-phase clouds containing supercooled liquid water (SLW) over the SO than at equivalent latitudes in the Northern Hemisphere (Chubb et al., 2013; Morrison et al., 2011), and recent in situ observations confirmed the ubiquity of supercooled liquid clouds and lack of ice to -20° C (McFarquhar et al., 2021). In situ observations, although limited, also indicate more frequent drizzle and less ice over the SO compared to Arctic supercooled and mixed-phase clouds (Chubb et al., 2013). Despite observed

MOORE ET AL. 1 of 20

Formal analysis: Kathryn A. Moore, Thomas C. J. Hill, Christina S. McCluskey, Cynthia H. Twohy, Bryan Rainwater, Darin W. Toohey, Kevin J. Sanchez

Funding acquisition: Thomas C. J. Hill, Cynthia H. Twohy, Darin W. Toohey, Sonia M. Kreidenweis, Paul J. DeMott Investigation: Kathryn A. Moore, Thomas C. J. Hill, Christina S. McCluskey, Cynthia H. Twohy, Bryan Rainwater, Darin W. Toohey, Kevin J. Sanchez, Paul J. DeMott

Methodology: Kathryn A. Moore, Thomas C. J. Hill, Paul J. DeMott Resources: Sonia M. Kreidenweis, Paul J. DeMott

Software: Kathryn A. Moore, Thomas C. J. Hill

Supervision: Sonia M. Kreidenweis, Paul J. DeMott

Validation: Kathryn A. Moore, Thomas C. J. Hill

Visualization: Kathryn A. Moore Writing – original draft: Kathryn A. Moore

Writing – review & editing: Kathryn A. Moore, Thomas C. J. Hill, Christina S. McCluskey, Cynthia H. Twohy, Bryan Rainwater, Darin W. Toohey, Kevin J. Sanchez, Sonia M. Kreidenweis, Paul J. DeMott differences between SO and Northern Hemisphere clouds, almost all model parameterizations have been developed with Northern Hemisphere data due to the lack of direct observations over the SO (Bromwich et al., 2012).

Until recently, earth system models, including those participating in CMIP5 (Coupled Model Intercomparison Project Phase 5), and reanalysis products overestimated the occurrence of ice and had insufficient liquid cloud cover over the SO, leading to a large shortwave radiation bias in the region (Bodas-Salcedo et al., 2013; Gettelman et al., 2020; Kay et al., 2016a, 2016b; Naud et al., 2014). This imbalance was hypothesized to be due to over-prediction of cloud glaciation and ice precipitation processes (Frey & Kay, 2017; Kay et al., 2016a; Mace et al., 2020; McFarquhar et al., 2021; Tan et al., 2016; Vergara-Temprado et al., 2018). Improvements in individual CMIP6 (Coupled Model Intercomparison Project Phase 6) models increased SLW and reduced radiation biases, improving agreement with observations (Bodas-Salcedo et al., 2019; Gettelman et al., 2020). Updated model representations of clouds are also responsible for higher equilibrium climate sensitivities (ECS) in many CMIP6 models compared to their CMIP5 counterparts due to corresponding changes in shortwave cloud forcing, likely driven by increases in SLW in CMIP6 models (Zelinka et al., 2020). The cloud phase feedback over the SO is anticipated to strongly influence simulated future ECS (Bjordal et al., 2020), so understanding processes that affect cloud phase in this region is critical.

Cloud condensation nuclei (CCN) and ice nucleating particle (INP) budgets and sources for the SO are not fully constrained, although the dominant source for CCN is local (Humphries et al., 2021; Quinn et al., 2017; Twohy et al., 2021). The typically small droplet numbers of low marine clouds make them sensitive to changes in aerosol concentration, size, and source. Low INP concentrations, coupled with scavenging and deposition in drizzle, can limit primary ice production and contribute to high supercooling in liquid and mixed phase clouds. This has been observed in several marine regions in the Northern Hemisphere (Rosenfeld et al., 2013), and may also be occurring in the SO. Vergara-Temprado et al. (2018) provided support for this hypothesis using the United Kingdom Met Office Global Unified Model, based on modeled INP concentrations. Secondary ice production has been observed in SO clouds >-25°C, with sometimes large discrepancies between measured ice crystal and INP number concentrations. However, a large proportion of clouds do not contain measurable ice concentrations (Järvinen et al., 2022). These observations indicate INPs may potentially play a large role in SO cloud phase, with downstream effects including cloud lifetime, precipitation, radiation budgets, and even ECS.

Historically, INPs have been thought of as large, insoluble particles with surface structures that have specific sites that promote the freezing of ice (Pruppacher & Klett, 2010). These sites, known as active sites, typically scale with particle surface area and so are more numerous in larger particles (see Kanji et al., 2017). This approach has been used to derive model parameterizations for ice nucleation as a function of activation temperature by normalizing INP concentrations with a more commonly measured value, such as particle surface area or number concentration (e.g., DeMott et al., 2010, 2015; Hoose & Möhler, 2012; Kanji et al., 2017; McCluskey et al., 2018c; Niemand et al., 2012; Ullrich et al., 2017). This approach requires the aerosol type or mixture to be known, since INP efficiency varies widely among particles of differing composition (e.g., Kanji et al., 2017). Strong relationships between INP concentrations and particles $>0.5 \mu m$ have been observed for mineral dust (DeMott et al., 2015), which is supported by the dominant supermicron mode of mineral and soil dust size distributions (Maring et al., 2003). Increasing awareness and study of additional categories of INPs, such as biological ice nucleators, which can be soluble and/or as small as $\sim 10 nm$, has challenged these assumptions about INP prerequisites (e.g., Kanji et al., 2017; O'Sullivan et al., 2015; Pummer et al., 2015; Wilson et al., 2015).

On a global scale, mineral and soil dusts are the dominant heterogeneous INP types in the immersion freezing mode due to their efficient ice nucleating ability (Hoose & Möhler, 2012; Testa et al., 2021) and high emission rates (Ginoux et al., 2012). Marine INPs have been identified as a distinct category (see DeMott et al., 2016), and shown to include marine diatoms and their exudates (Rosinski et al., 1987; Wilson et al., 2015), as well as marine macromolecules (McCluskey et al., 2018b). Very recent laboratory studies indicate supermicron aerosol may be an important marine INP (Mitts et al., 2021), however, no assessment of the atmospheric transport of such particles was conducted and ambient observations have yet to confirm this. Marine INP number concentrations are generally 2–3 orders of magnitude or more lower than continental measurements (DeMott et al., 2016), as are marine INP active site densities (McCluskey et al., 2018c).

Measurements of SO INPs are sparse, with initial measurements conducted by Bigg (1973, 1990), and the remainder comprised of data from several cruises, one aircraft campaign, and one study at the Australian Antarctic Division's Macquarie Island station, all in the last decade (Kremser et al., 2021; McCluskey et al., 2018a;

MOORE ET AL. 2 of 20

McFarquhar et al., 2021; Miyakawa et al., 2023; Schmale et al., 2019; Tatzelt et al., 2022; Welti et al., 2020). Many of the measurements were also limited to the surface and to INPs active at temperatures of -15 or -20° C due to either instrumental constraints or a particular focus on warmer mixed phase clouds (Welti et al., 2020). There is now a consensus, supported by the observed low INP numbers, its remote location, and modeling studies (Burrows et al., 2013; McCluskey et al., 2019; Vergara-Temprado et al., 2017), that the SO INP population in the MBL is dominated by sea spray aerosol (SSA) and distinct from that found in the Northern Hemisphere. This is unlike the northern high latitudes, where mineral dust has been shown to dominate over locally sourced marine INPs in regions such as the Canadian Arctic (Irish et al., 2019).

2. Methods

2.1. Southern Ocean Measurement Campaigns

Measurements presented in this study were collected during the Southern Ocean Cloud Radiation Aerosol Transport Experimental Study (SOCRATES, hereafter SOC) aircraft campaign and the second Clouds, Aerosols, Precipitation, Radiation and atmospherIc Composition Over the Southern Ocean (CAPRICORN-2, hereafter CAP-2) ship campaign. Both campaigns were conducted simultaneously during Austral summer (January–March) 2018, based out of Hobart, Tasmania and are fully described in McFarquhar et al. (2021). SOC measurements utilized the National Science Foundation (NSF)/NCAR G-V aircraft (UCAR/NCAR—Earth Observing Laboratory, 2005) and collected cloud microphysical and aerosol observations within the MBL and up to the free troposphere as far south as 62°S. CAP-2 collected complementary MBL measurements aboard the RV *Investigator* (voyage IN2018_V01), an Australian Government research platform operated by the Commonwealth Science and Industrial Research Organization (CSIRO). A map indicating the locations of the 15 SOC research flights and the CAP-2 track are given in Figure S1 in the Supporting Information S1. The SOCRATES campaign is noteworthy for collecting the first in situ observations of INPs in and above cloud in this region.

2.2. Aerosol Measurements

The collection and analysis of particle size distribution measurements during CAP-2 and SOC were fully described in Moore et al. (2022) and will only be briefly covered in Text S1 in Supporting Information S1 (CAP-2 size distributions), Text S2 in Supporting Information S1 (SOC size distributions), and Text S3 in Supporting Information S1 (SOC aerosol composition). Integrated particle number, surface area, and volume concentrations are used as normalization metrics and inputs to parameterizations for estimating INP concentrations, as discussed in Section 3.2. Measurements of single particle composition during SOC using offline elemental analysis (Twohy et al., 2021) are similarly used as parameterization inputs (Section 3.4).

2.3. Ice Nucleating Particle Observations

Measurements of INPs active in the immersion freezing mode were made in real time with Colorado State University (CSU) Continuous Flow Diffusion Chambers (CFDCs) at temperatures below -25° C, and via offline analyses of aerosol filter samples using the CSU Ice Spectrometer (IS) from -10 to -30° C. Ice crystals that activated within the CFDC were also collected and analyzed by STEM/EDS to assess the composition and size of INP residuals (Twohy et al., 2021).

2.3.1. Continuous Flow Diffusion Chamber Measurements

The CFDC is an online instrument used to measure primary INP number concentrations in an aerosol stream (DeMott et al., 2015; Rogers, 1988; Rogers et al., 2001). Two concentric, cylindrical walls are coated with ice and thermally controlled to establish a temperature and humidity gradient between the walls in the upper "growth" region of the chamber, allowing aerosol particles to activate into ice crystals and grow. The HIAPER (CFDC-1H) version of the CFDC used in SOC (Barry et al., 2021) and a duplicate version used during CAP-2 (McCluskey et al., 2018a) both have total residence times of ~7 s based on their sample volumetric flow rate of 1.5 lpm. Ice crystals are detected optically with an optical particle counter (OPC) at the base of the chamber and distinguished by size from aerosol or activated cloud droplets. For both SOC and CAP-2, water supersaturated conditions, typically 104%–108% RH, were maintained in the growth region, which forces activation of aerosols into cloud droplets prior to ice nucleation, giving results similar to offline immersion freezing techniques (DeMott et al., 2016).

MOORE ET AL. 3 of 20

Prior to entering the chamber, the aerosol stream is dried to below the frost point, and supermicron aerosols that might interfere with optical detection of ice crystals are removed by passing the aerosol stream through two identical single-jet impactors in series. For SOC, impactors with a 2.4 μm cut size were used; during CAP-2 1.5 μm impactors were used to limit interferences from highly hygroscopic, supermicron sea spray aerosols. Low INP concentrations during both campaigns limited operating temperatures to −25°C and below, with the majority of measurements collected ~−30°C. Measurement periods of approximately 10 min were alternated with 5-min periods measuring HEPA-filtered air to provide instrument background counts, which vary by operating temperature and environmental conditions. INP concentrations presented here have been background-corrected using adjacent filtered-air periods, as described in Barry et al. (2021) and Moore (2020). Calculation of confidence intervals and assessment of statistical difference between sample and background periods follow Krishnamoorthy and Lee (2012) and are also detailed in Barry et al. (2021) and Moore (2020). Concentrations are reported at standard conditions (STP; 0°C and 100 kPa).

During CAP-2, the CFDC sampled from the same RV Investigator aerosol sampling inlet as the SMPS, APS, and other aerosol instrumentation (Moore et al., 2022). In addition to direct ambient measurements, an aerosol concentrator (MSP Corporation Model 4240) was employed upstream of the CFDC to pre-concentrate ambient aerosol and enhance INP number concentrations prior to measurement, as in previous ground-based (Tobo et al., 2013) and ship-board (McCluskey et al., 2018a) studies. The aerosol concentrator inlet was constructed from 1 inch stainless steel tubing and followed the same path as the main aerosol inlet down the RV Investigator foremast and into the aerosol lab at the bow of the ship. INP concentration factors for measurements made with the aerosol concentrator were calculated through comparison to ambient INP measurements made at the same temperature $(\pm 2^{\circ}\text{C})$ and within 30 min. These concentration factors were used to scale measurements made with the aerosol concentrator to their equivalent ambient concentration. Theoretical particle transmission efficiency calculations for the CFDC ambient and concentrator inlets (Figure S3 in Supporting Information S1; Brockmann, 2011; von der Weiden et al., 2009) indicate >90% for the ambient and >85% transmission efficiency for the concentrator inlet at sizes up to 1.5 μm, and so no particle loss corrections were applied to measured INP concentrations. Unlike the aerosol size distribution measurements (Text S1 in Supporting Information S1), the CFDC data were not filtered to exclude ship exhaust, as previous measurements have indicated very low IN efficiency of particles emitted from diesel engines (Schill et al., 2016), and inspection of INP concentrations showed no significant differences between adjacent measurements when one was influenced by ship exhaust and the other was not. This is consistent with previous ship-board measurements for temperatures above -26°C (Irish et al., 2019; McCluskey et al., 2018a; Welti et al., 2020).

On the G-V, the CFDC sampled from both the HIAPER modular inlet (HIMIL inlet; Stith et al., 2009) in clear air regions above and below clouds, and from a counterflow virtual impactor (CVI) inlet within clouds (Noone et al., 1988; Twohy et al., 2010) to detect INPs within cloud residuals. Particle transmission efficiencies for the HIMIL inlet have been previously characterized as >94% for submicron particles (Stith et al., 2009), and no corrections were applied to the CFDC data, which has an upper limit of 2.4 µm aerodynamic diameter. CVI transmission efficiencies were modeled by Twohy et al. (2010) using computational fluid dynamics software, and used to correct the in-cloud CVI data presented here for particle enhancements in the inlet. Some measurements in cloud-adjacent regions were also made using the CVI inlet in clear air, with the counterflow turned off ("total mode"). CVI enhancements in total mode are highly size dependent, and expected to range from ~1.1 to 3.5 for the particle sizes sampled by the CFDC (Twohy et al., 2016). Since INP sizes during each measurement are unknown, but likely variable (Twohy et al., 2021), no correction has been applied to the total mode CVI measurements from SOCRATES.

2.3.2. Ice Spectrometer Measurements

Aerosols were collected onto pre-cleaned $0.2~\mu m$ pore size, 47~mm diameter track-etched polycarbonate membrane filters (Whatman Nucleopore filters, GE Healthcare Life Sciences) in either pre-sterilized aluminum inline filter housings (Pall) on the G-V, or disposable, sterile, open-faced filter units (Nalgene sterile analytical filter units, Thermo Fisher Scientific) on the RV *Investigator*. During CAP-2, filters were mounted on deck beneath a rain hat for alternating 24 and 48 hr periods at approximately 23 m above sea level. In order to limit ship exhaust contamination, the filter pump was powered with a sector sampler, which provided power to the pump only when the wind speed relative to the ship was between 10 and 80 knots, the ship-relative wind direction was from the forward 90° (relative wind directions greater than 45° and less than 315° were excluded), and the

MOORE ET AL. 4 of 20

total particle concentrations measured by a condensation particle counter (CPC; TSI 3010) were stable and less than $2,000~\rm cm^{-3}$. On the G-V, filters sampled from the same HIMIL as the CFDC (Section 2.3.1) above or below cloud. Due to the low INP concentrations, each SOC filter was collected for multiple, approximately level legs at similar altitudes, but different locations throughout a flight. Separate filters were collected in the MBL and above cloud to assess changes in INPs with altitude. Filters where >5% of the collection period was in-cloud based on cloud condensed water measurements (Text S2 in Supporting Information S1) have been excluded from results presented here. Filters were stored frozen (-80° C) following collection and during transport (via a liquid nitrogen dry shipper) back to CSU, and at -20° C thereafter. Blank filters were collected throughout the voyage and during the research flights and processed identically to the samples. Details on filter collection location, time, and accumulated volumes are given in Table S2 in Supporting Information S1 for CAP-2 and Table S3 in Supporting Information S1 for SOC.

The CSU IS was used to measure immersion freezing INP temperature spectra from liquid suspensions of particles collected onto filters during CAP-2 and SOC. The current version of the IS was described in DeMott, Möhler et al. (2018) and Hiranuma et al. (2015). Aliquots of sample suspensions, typically 32 or 48 droplets of 50 μ L, were dispensed into sterile 96-well PCR trays (Optimum Ultra, Life Science Products) and then placed into temperature-controlled aluminum blocks and cooled at approximately 0.33°C min⁻¹. Freezing was detected optically using a CCD camera, with the number and position of frozen droplets (wells) recorded at 1 Hz. The minimum analysis temperature for each sample or blank was determined by comparison with a 0.1 μ m-filtered DI water negative control and was typically between -27 and -30°C. Calculations of INP concentrations in the liquid suspension were made following Vali (1971), which were then converted to concentrations in ambient air, expressed at standard conditions (STP; 0°C and 100 kPa). Uncertainties are reported as binomial sampling confidence intervals (95%) as in Agresti and Coull (1998). The limit of detection (LOD) was taken as the upper 95% confidence interval for 0 droplets frozen out of a sample, corresponding to 3–4 frozen wells for these filter collections. As a result, samples were considered above the LOD once 4–5 wells had frozen, leading to an upper temperature limit of about -17°C. Measured concentrations were corrected using the average background number of INPs from 6 (SOC) or 5 (CAP-2) blank filters and are not reported if blank-corrected values fell below zero.

An earlier version of the SOC IS filter data set was presented in Järvinen et al. (2022) as a comparison to in-cloud measurements of ice crystal number concentrations, and the concentrations were used in McCluskey et al. (2023) and Zhao et al. (2023) to evaluate model INP predictions (Section 2.4, Text S4 in Supporting Information S1). Preliminary CAP-2 filter results were shown in McFarquhar et al. (2021), along with previous measurements made in the SO. The blank-correction procedure reported here represents an improved statistical methodology from what has been previously reported (e.g., Barry et al., 2021; DeMott, Möhler, et al., 2018), providing more accurate 95% confidence intervals on blank-corrected data and improved LOD estimations. The midpoint concentrations are identical to previous methodologies and are directly comparable.

2.3.3. INP Size and Composition Analysis

Following the OPC at the outlet of the CFDC chamber is a single-jet impactor with a 50% cut-size of 4 μ m aerodynamic diameter, which was used to collect ice crystals that nucleated inside the CFDC chamber during both SOCRATES and CAPRICORN-2 (Barry et al., 2021; McCluskey et al., 2014). Similarly to the total particle collections during SOC (Text S3 in Supporting Information S1), the CFDC STEM impactor was fitted with Cu grids (coated with formvar and C), and the collected ice crystal residuals were analyzed with STEM/EDS to determine residual size, morphology, and composition (Twohy et al., 2021). In this study, only the size measurements of INPs will be discussed. Six samples from CAP-2 and four samples from SOC were collected, with collection temperatures that ranged from -27 to -32°C and n = 87 total particles analyzed; the collection locations are shown in Twohy et al. (2021); Figure 1. Since all the CAP-2 and the majority of the SOC INPs were collected in the MBL, the overall sample is expected to be dominated by particles from the MBL.

Indirect inference of INP sizes was also possible based on the INP concentration factors calculated from CAP-2 ambient CFDC measurements versus those made using the aerosol concentrator (Section 2.3.1). The aerosol concentrator primarily acts on particles >0.5 μ m diameter, with a concentration factor that is highly size dependent up to ~1 μ m aerodynamic diameter (Tobo et al., 2013). For particles 0.5–1 μ m aerodynamic diameter, the measured INP concentration factor thus provides indirect evidence of INP size. Due to the very low INP concentrations present over the SO MBL (Figure 1), measurements of INP concentration factor were limited to \leq -25°C,

MOORE ET AL. 5 of 20

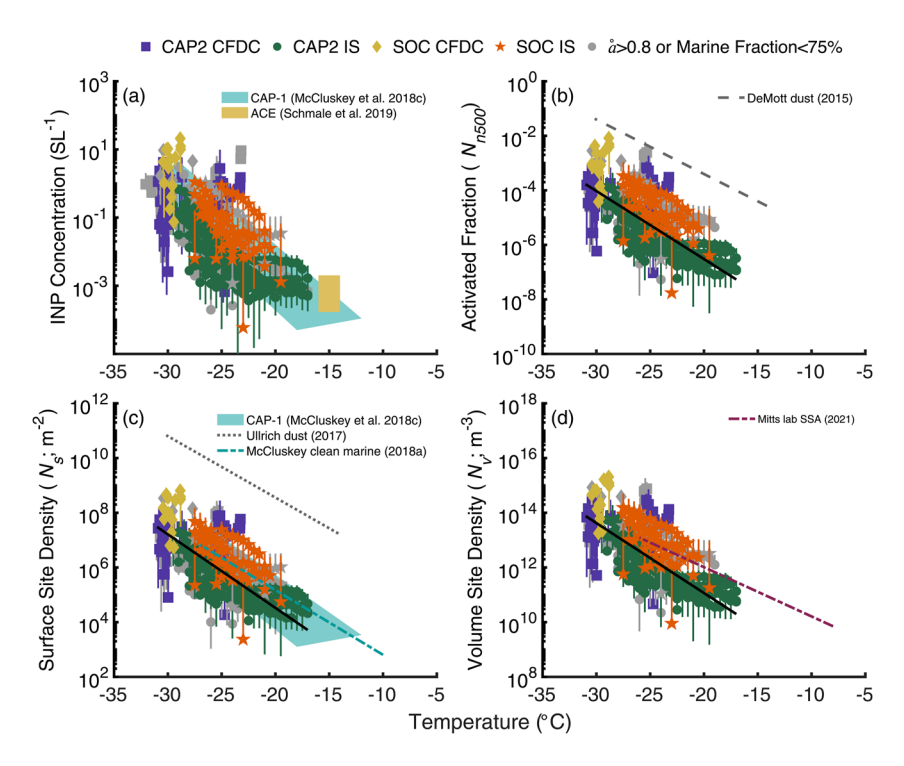


Figure 1. Ice nucleating particle (INP) (a) number concentration, (b) normalized by $n500~(N_{n500})$, (c) normalized by aerosol surface area (N_s) and (d) normalized by aerosol volume (N_v) temperature spectra during SOC and CAP-2 in the marine boundary layer (MBL). CAP-2 Continuous Flow Diffusion Chamber (CFDC) (purple squares), CAP-2 filter (green circles), SOC CFDC (gold diamonds), and SOC filter (orange stars) are shown in (a), and in (b)–(d) when simultaneous aerosol observations were available for normalization. In (a) and (c), the blue shading indicates the range of values observed during CAPRICORN-1 (McCluskey et al., 2018a). The gold shading in (a) shows observations made during the Antarctic Circumnavigation Expedition (ACE) campaign (Schmale et al., 2019). In (b), the gray dashed line shows the DeMott et al. (2015) parameterization for dust based on n500, using the mean n500 value observed during CAP-2. In (c), the gray dotted line indicates the Ullrich et al. (2017) parameterization for dust N_s , and the blue dot-dash line shows the N_s parameterization from McCluskey et al. (2018c) for North Atlantic clean marine air. The dashed magenta line in (d) indicates the Mitts et al. (2021) lab-based parameterization for marine N_v . Non-gray symbols have an $a \le 0.8$ and 5-day back trajectory ocean fraction >75% to identify samples dominated by marine aerosol; gray symbols do not meet at least one of these criteria. Solid black lines in (b)–(d) indicate the best-fit exponential functions (Equation 1, Table S1 in Supporting Information S1) to the non-gray symbols.

and predominantly $\sim -30^{\circ}$ C. Concentration factors of the aerosol concentrator as a function of particle diameter were derived from sequential measurements of ambient aerosol particles with and without the aerosol concentrator upstream of an Aerodynamic Particle Sizer (TSI, APS 3321) for particles between 500 nm and 20 μ m aerodynamic diameter. They are shown in Figure 5, where the particle sizes have been converted from aerodynamic to physical dry diameter, using the APS diameter correction factor derived for CAP-2 particle measurements (Moore et al., 2022).

2.4. SOCRATES CAM6 Model Simulations

A simulation of aerosols during SOCRATES was conducted with the atmospheric component of CESM2 (Community Earth System Model version 2), CAM6 (Community Atmosphere Model version 6), as described and presented in McCluskey et al. (2023). Additional details on the simulation are presented in Text S4 in Supporting Information S1. McCluskey et al. (2019, 2023) concluded the best approach for predicting INP concentrations over the SO using CAM and existing parameterizations was to sum the sea spray INP contribution using the marine organic aerosol parameterization (M18) from McCluskey et al. (2018c) and the mineral dust INP contribution following the DeMott et al. (2015) parameterization (D15). The simulated CAM6 INP concentrations presented in this study use this approach. Simulated sea salt aerosol surface area concentrations and the number concentration of mineral dust particles larger than 500 nm were used as parameterization inputs for M18 and D15, respectively.

MOORE ET AL. 6 of 20

3. Results and Discussion

3.1. CAPRICORN-2 and SOCRATES Marine Boundary Layer INP Observations

The most comprehensive historical measurements of SO INPs are those of Bigg (1973, 1990). Since then, measurements of INPs, primarily immersion freezing assays of aerosol filters, have been collected during several campaigns in different regions of the SO, and are collated in McFarquhar et al. (2021) and Welti et al. (2020). As previously noted for the CAPRICORN-1 (2016; McCluskey et al., 2018a) and Antarctic Circumnavigation Expedition (ACE, 2016–2017; Schmale et al., 2019; Tatzelt et al., 2022; Welti et al., 2020) campaigns, modern measurements are one to several orders of magnitude lower than the original observations presented in Bigg (1973). During CAP-2, average IS measurements of filters at -20° C are approximately 2 orders of magnitude lower than those collected during 1969–1972 across all latitudes sampled. Measurements at temperatures above -15° C from CAP-2 were below the detection limit, which prevents additional direct comparisons. Slightly elevated INP concentrations were observed at -25° C during CAP-2 at the northern and southern ends of the voyage (not shown), though all latitudinally-averaged values agree within their estimated uncertainties. Future measurements should evaluate this latitudinal variability during seasons other than austral summer.

INP measurements collected in the MBL from both IS filters and CFDC observations during SOCRATES and CAPRICORN-2 are compiled in Figure 1. As discussed in Section 2.3.2, the INP filter measurements included in this study represent updated versions of the data sets, with improved confidence interval and LOD estimates. All panels in Figure 1 show INP observations as a function of temperature; Figure 1a has measured INP concentrations and the remaining panels display INP concentrations normalized by measured aerosol concentration metrics for comparison to model parameterizations, which will be discussed further in Section 3.2. Normalization of INP concentration with particle number gives activated fraction, N_n (Figure 1b), normalization with particle surface area gives the surface active site density, N_s (Figure 1c), and normalization with particle volume gives the volume active site density, N_v (Figure 1d). The activated fraction presented in this study uses the number concentration of aerosols larger than 500 nm (n500), which has been used in several previous INP model parameterizations (e.g., DeMott et al., 2015; Tobo et al., 2013). While the surface active site density is typically abbreviated as n_s , will be used throughout this manuscript to distinguish it from n500. Best-fit exponential functions (black lines in Figures 1b–1d) are given by Equation 1:

$$N_x(T) = \exp(a \cdot T + b) \tag{1}$$

where N_x is the activated fraction (N_{n500}), surface active site density (N_s), or volume active site density (N_v), T is temperature (°C), and a and b are fit parameters. Fit parameters and R^2 values for functions shown in Figure 1 are listed in Table S1 in Supporting Information S1. The median-lognormal fitting process suggested by Li et al. (2022) was attempted, but the relatively small number of available measurements at warm temperatures prevented robust estimates of the lognormal fit parameters. Instead, regression parameters were calculated with all the available data, using the least absolute residuals method to reduce the impact of extreme values far from the median (e.g., Bassett & Koenker, 1978).

Good agreement is seen with previously published INP measurements from the SO during the CAPRICORN-1 campaign (McCluskey et al., 2018a; blue shading in Figures 1a and 1c). Due to the more stringent blank-correction procedure applied to this IS data set than previous ones (Section 2.3.2), there is no direct overlap with the warm-temperature results from ACE (Schmale et al., 2019; gold shading in Figure 1a), although they are at the high end of those reported for CAPRICORN-1. Additional results from ACE presented in Tatzelt et al. (2022) and Welti et al. (2020) have not been included, as they were not corrected for field blanks, which are a significant fraction of the measured concentrations particularly at colder temperatures (Tatzelt et al., 2022, Figures S5 and S8). The lack of blank correction may also explain the higher INP concentrations reported from ACE measurements relative to those from CAPRICORN-1, CAP-2, and SOC, although differences in sampling time and location likely also play a role. Parameterizations for dust INPs based on global INP data and number concentrations of aerosols larger than 500 nm (DeMott et al., 2015) or aerosol surface area concentrations (Ullrich et al., 2017) overpredicted the observations from SOC and CAP-2, corroborating the growing consensus that the majority of boundary layer-INPs in this region are local, and of marine origin (Burrows et al., 2013; McCluskey et al., 2018a, 2019, 2023; Vergara-Temprado et al., 2017; Welti et al., 2020). The N_c-based marine INP parameterization proposed by McCluskey et al. (2018c) using data collected at Mace Head Research Station in Western Ireland is consistent with the exponential best-fit line derived using this data set between -25 and -27° C, but

MOORE ET AL. 7 of 20

has an increasing high bias at warmer temperatures. The more conservative blank-correction procedures used for this study relative to past campaigns (Section 2.3.2) may have contributed to the lower slope obtained by McCluskey et al. (2018c). Similarly, the Mitts et al. (2021) parameterization for N_{ν} based on laboratory measurements has a lower slope than the fit derived from this data set, and as a result was found to lie at or above the upper bound of CAP-2 and SOC measurements for temperatures warmer than -20° C, and above the best fit line at all temperatures.

Although there is overall agreement between the campaigns, the SOC filter and CFDC measurements in the MBL are offset toward warmer concentrations relative to those from CAP-2. There are a few likely explanations for this, including that the aircraft and ship were only infrequently targeting the same region, so the measurements represent two different samples of the overall SO MBL INP population. As detailed in McFarquhar et al. (2021), the SOC flights targeted (though not exclusively) the cold sectors of extratropical cyclones, as this is a category where models struggle to accurately simulate SLW abundance. In addition, instrument backgrounds on the aircraft were typically higher than on the ship, which prevented detection of very low concentrations during SOC. As seen in Figure S5 in Supporting Information S1 and further discussed in Section 3.2, the SOC observations had higher minimum and maximum wind speeds than were observed during CAP-2, which are associated with higher INP concentrations. Finally, it is possible some stratification occurred at low levels which influenced the aerosol vertical profiles. However, an analysis of the soundings collected during CAP-2 and SOC (McFarquhar et al., 2021) suggests the SO atmosphere was typically well-mixed to at least 900 hPa, which is well above the 150–300 m altitudes (Text S2 in Supporting Information S1) where the SOC MBL measurements were collected. A comparison of the few overflights of the RV Investigator by the G-V (example shown in Figure 7a and further discussed in Section 3.4) suggests that when the aircraft and ship were in the same location, the SOC and CAP-2 measurements agree extremely well.

The role of air-mass history and particle source on INP observations was explored using Ångström exponent (\hat{a} ; Moore et al., 2022) and HYSPLIT (Rolph et al., 2017; Stein et al., 2015) back trajectories. $\hat{a} \leq 0.8$ (Text S1 in Supporting Information S1) was previously found to work well as a tracer for aerosol size distributions dominated by primary marine aerosol during CAP-2, and was further supported by the degree of marine influence calculated from HYSPLIT back trajectories (Moore et al., 2022). The degree of marine influence was defined as the fraction of a 5-day back-trajectory that passed over the ocean (Sanchez et al., 2021). Non-gray points in Figure 1 have both $\hat{a} \leq 0.8$ and a HYSPLIT marine influence >75%; gray points did not meet at least one criterion to be considered marine-dominated. While these metrics worked well to classify SOC and CAP-2 aerosol measurements, there were no discernible differences in INP concentrations or normalized values for marine-dominated periods versus the remaining measurements. Similarly, using primary marine aerosol number, surface area, or volume (Figure S4 in Supporting Information S1) to normalize INP concentrations produced the same results as using total quantities.

3.2. Parameterizing Marine INP Concentrations

For marine INPs, two parameterizations based on field measurements have been published; one uses aerosol surface area (M18; McCluskey et al., 2018c), and the other SSA organic carbon mass (W15; Wilson et al., 2015) to predict INP concentrations, in addition to activation temperature. The TOC-based parameterization of Wilson et al. (2015) used INP measurements and organic carbon mass concentrations of sea surface microlayer samples from the Arctic and North Atlantic Oceans to estimate INPs in the organic component of SSA. W15 was evaluated in McCluskey et al. (2018c) for North Atlantic marine atmospheric INPs and found to overpredict INP concentrations at -15 and -20°C by a factor of 4-100. Using the same observations, M18 developed an alternative parameterization based on measurements of ambient INPs in SSA at Mace Head, Ireland, which specifically aims to describe organic-coated sea salt particles and not INPs active at warm temperatures, which may be associated with microbes. Both W15 and M18 were evaluated using E3SMv1 (Energy Exascale Earth System Model version 1) simulations of INPs during the March 2016 to March 2018 Macquarie Island Cloud Radiation Experiment (MICRE) campaign (Raman et al., 2023). Unlike for the CAPRICORN-1 and SOCRATES campaigns (McCluskey et al., 2019, 2023), W15 produced the best agreement with the MICRE atmospheric INP observations (DeMott, Hill, Marchand, & Alexander, 2018; McFarquhar et al., 2021). However, MICRE observations were also found to be higher than those from open ocean SO measurements, including during ACE (Tatzelt et al., 2022) and the Measurements of Aerosols, Radiation, and Clouds over the SO (MARCUS)

MOORE ET AL. 8 of 20

campaign (DeMott, Hill, & McFarquhar, 2018; McFarquhar et al., 2021). This discrepancy is likely due to local processes enhancing INP concentrations at Macquarie Island (Raman et al., 2023). Microlayer samples analyzed in W15 varied in ice nucleation activity, with those from the North Atlantic generally having lower concentrations than those in the Arctic. As a result, W15 North Atlantic samples may be more consistent with the open-ocean measurements from McCluskey et al. (2018a) during CAPRICORN-1 and those presented here from CAP-2 and SOC. Since SOC and CAP-2 measurements are in good agreement with those from CAPRICORN-1, and W15 predicts higher INP concentrations than M18, we adopt the approach of McCluskey et al. (2019, 2023) and use M18 instead of W15 here. Very recent laboratory experiments suggest that for marine INPs, the active site density may be proportional to particle volume rather than surface area (Mitts et al., 2021), however, field confirmation of this is lacking.

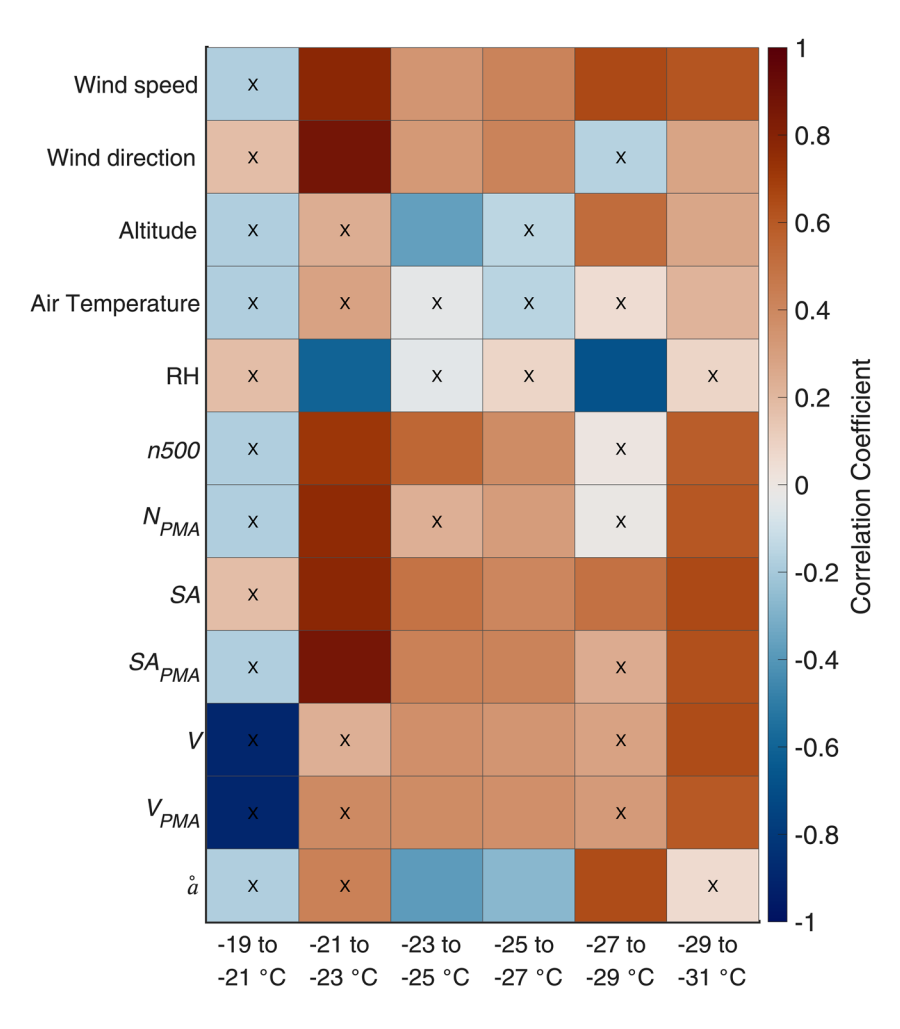
The utility of different normalizations for predicting INP concentrations over the SO are demonstrated in Figure 1. Measurements from CAP-2 and SOC collected in the MBL were normalized by the number of particles larger than 500 nm $(N_{n500}$; Figure 1b), aerosol surface area $(N_s$; Figure 1c) and aerosol volume $(N_v$; Figure 1d) when simultaneous aerosol measurements were available. While aerosol surface area reduced the spread (in orders of magnitude) of observations the most, none of the normalizations applied here capture the variability in observed INP concentrations. This suggests parameterizations exclusively based on aerosol physical characteristics are only modestly useful in predicting marine INP concentrations, as also concluded by Tatzelt et al. (2022). To further investigate possible INP parameterization inputs, a Spearman's rank correlation analysis was performed between selected environmental variables, aerosol physical characteristics, and concentrations of INPs in binned temperature ranges; the results are shown in Figure 2. No strong correlation was found between a single environmental or aerosol metric that applied for every temperature range of INPs, however, moderate but significant correlations (p < 0.05) were found with both wind speed and aerosol surface area for temperatures colder than -21°C. Tatzelt et al. (2022) performed a similar analysis between ACE INP concentrations and aerosol number and mass, but did not find any significant relationships between INP and aerosol measurements. However, it should be noted that they did not test for correlations with aerosol surface area, and they only had one INP measurement temperature colder than −21°C.

SSA concentrations are known to increase with wind speed due to enhanced aerosol formation through wave breaking and bubble bursting (e.g., O'Dowd & de Leeuw, 2007). This relationship was also observed for INP concentrations in the MBL during SOC and CAP-2 (Figure 3, Figure S5a in Supporting Information S1). INP data used in Figure S5 in Supporting Information S1 were limited to INPs active at temperatures <-27°C to reduce the influence of temperature on the observed relationship, since freezing temperature exerts an outsized impact on measured INP concentrations. The wind speed range for the INP measurements shown in Figure S5 in Supporting Information S1 was 4-23 m s⁻¹, which covers the majority of the observed range in the MBL during CAP-2 (0.1–28 m s⁻¹), though it should be noted measurements were limited to austral summer. Previous research into marine INPs has focused on organic and biological species (e.g., DeMott et al., 2016; McCluskey et al., 2018b, 2018c; Wilson et al., 2015), as soluble salts are not expected to contribute to heterogeneous ice nucleation in the immersion freezing mode, which is the most relevant nucleation mode for low and mixed-phase clouds (e.g., Kanji et al., 2017). Although limited to coastal measurements in the North Atlantic and North Pacific, Gantt et al. (2011) found the organic mass fraction of SSA was inversely correlated with wind speed. Taken together, this would predict, if anything, negative correlations between normalized marine INP concentrations and wind speed. However, normalizing the INP concentrations by n500, aerosol surface area, or aerosol volume (Figures S5b-S5d in Supporting Information S1) did not remove the positive wind speed dependence, even though all three aerosol parameters are themselves positively correlated with wind speed (Moore et al., 2022). Figure 3 demonstrates that the positive correlation between INP concentration and wind speed extends across the full INP temperature range measured during SOC and CAP-2 and was similarly unaffected by normalization. Together, Figure S5 in Supporting Information S1 and Figure 3 suggest marine INP emissions are not strictly proportional to SSA production, but instead are enhanced at higher wind speeds through an unknown mechanism. This finding may help explain why parameterizing marine INPs based solely on aerosol physical parameters has not explained as much of the observed variability as for other INP types, particularly dust.

One possible explanation for the observed positive relationship is the re-emission of deposited dust from the ocean surface during bubble bursting, which would be expected to increase with wind speed, similarly to supermicron SSA (e.g., O'Dowd & de Leeuw, 2007). Oceanic dust ejection has been postulated as a possible mechanism to influence atmospheric INP concentrations in remote marine regions, and particularly the SO on the

MOORE ET AL. 9 of 20

21698996, 2024. 2, Downloaded from https://agupubs.onlinelibrary.wiley.com/doi/10.1029/2023JD039543 by University Of California, Wiley Online Library on [06/02/2024]. See the Terms and Conditions (https://online



INP Temperature Range

Figure 2. Spearman's rank correlation between environmental variables, aerosol metrics, and concentrations of ice nucleating particles (INPs) in multiple temperature ranges. Correlation coefficient is indicated by color; boxes without crosses represent a significant relation (p < 0.05). Aerosol metrics tested include the number concentration of particles larger than 500 nm (n500), number concentration of primary marine aerosol ($N_{\rm PMA}$), total aerosol and PMA surface area concentration (SA and SA_{PMA}, respectively), total aerosol and PMA volume concentration (V and $V_{\rm PMA}$, respectively), and Ångström exponent (\mathring{a} ; 450/635 nm wavelength pair). Environmental variables include wind speed, wind direction, measurement altitude, and air temperature.

basis of lab experiments (Cornwell et al., 2020), though field confirmation is lacking. The preferential emission of INPs in spume droplets, which are generated by the tearing of wave crests at increasing rates for wind speeds above 9 m s⁻¹ (Monahan et al., 1986; Sofiev et al., 2011) is another possibility, although the droplets produced are predominantly >10 μ m. Finally, although the organic mass fraction tends to decrease at high wind speeds (Gantt et al., 2011), it is possible ice nucleation active organics are over-represented, which similarly requires further study.

Given the unexpected relationship found between INP concentrations and wind speed, we tested whether adding wind speed as an additional variable improved the marine INP parameterization developed by McCluskey et al. (2018c). Following the approach of Niemand et al. (2012), N_s for SO marine INPs was parameterized using an exponential relationship to activation temperature, with an additional exponential term for wind speed:

$$N_s(T, u) = \exp(a \cdot T + b) + \exp(c \cdot u + d) \tag{2}$$

where N_s is the surface active site density (m⁻²), T is temperature (°C), u is horizontal wind speed (m s⁻¹), and a, b, c, and d are fit parameters. CAP-2 and SOC data used to derive the fit parameters were limited to the non-gray

MOORE ET AL. 10 of 20

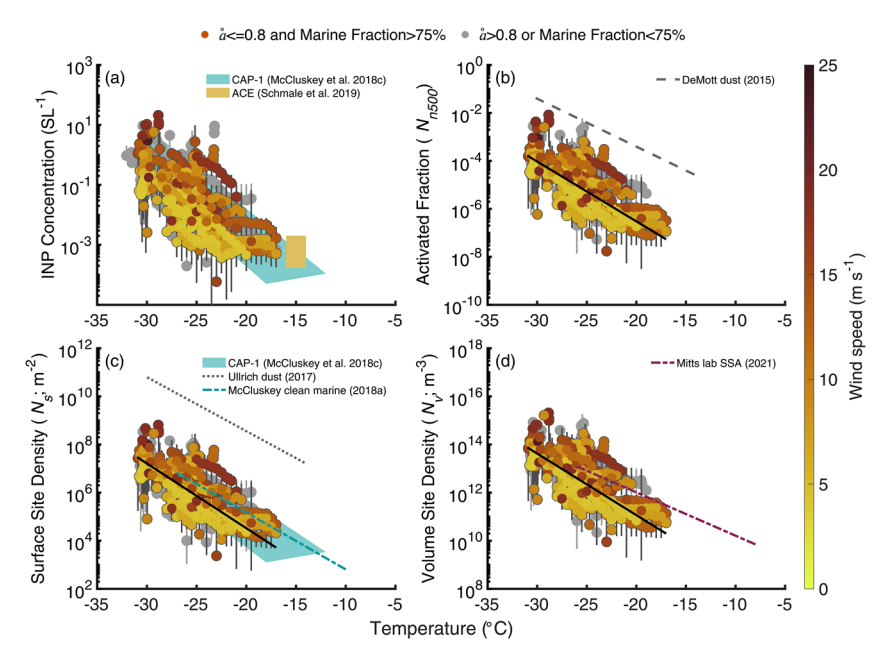


Figure 3. Ice nucleating particle (INP) (a) concentration, (b) N_{n500} , (c) N_s and (d) N_v temperature spectra during SOC and CAP-2 in the marine boundary layer. All Continuous Flow Diffusion Chamber and filter measurements are shown as circles and colored by the average wind speed during each measurement period. The shading, parameterizations, best-fit lines, and marine aerosol classification are identical to Figure 1.

points shown in Figure 3, namely, data collected within the MBL and with $a \le 0.8$ and 5-day back trajectory ocean fraction >75% to isolate marine aerosol. The fit parameters were determined to be: $a = -0.66 \pm 0.17$, $b = -3.11 \pm 5.11$, $c = 0.51 \pm 0.09$, and $d = 6.75 \pm 2.03$ for this data set. Modified normalized mean bias (B_n)

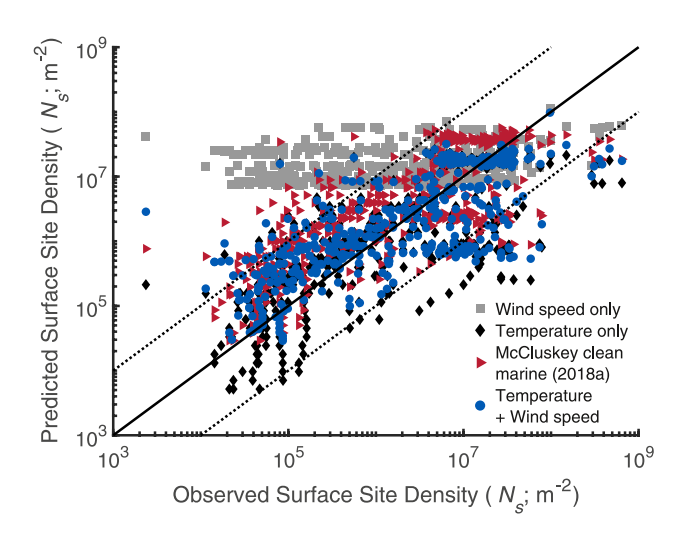


Figure 4. Predicted versus observed N_s during CAP-2 and SOC. Data shown are all from the marine boundary layer and are limited to observations with $\mathring{a} \leq 0.8$ and 5-day back trajectory ocean fraction >75% to isolate marine aerosol. Black diamonds show a single-exponential fit using only temperature $(B_n = -0.18)$, and gray squares only wind speed $(B_n = 1.07)$. Blue circles show a 2-exponential fit (Equation 2) to both wind speed and temperature $(B_n = 0.09)$. Red triangles use the N_s parameterization from McCluskey et al. (2018c) for clean marine air $(B_n = 0.54)$. The solid black line indicates a 1:1 relationship, and a factor of 10 deviation is shown by the dashed black lines.

was reduced from 0.54 to -0.18 by using the best-fit exponential to the SOC and CAP-2 MBL data instead of the parameterization derived from the North Atlantic (M18), as anticipated by the different slopes seen in Figure 1c. Using wind speed alone to predict N_s does a poor job reproducing the observations, with an increased bias $B_n = 1.07$ (Figure 4). Wind speed and temperature together performed the best, with a bias $B_n = 0.09$. The large range of INP concentrations (Figure 1) observed during CAP-2 and SOC are challenging to predict, but the results presented here suggest variables that have not previously been considered, including wind speed, may act as drivers of INPs. Further study is needed to fully understand the complex processes impacting INP concentrations and their variability.

3.3. Southern Ocean Marine INP Size

As discussed in Section 2.3.3, both direct and indirect measurements of INP size were conducted during SOC and CAP-2, based on electron microscopy analysis of ice crystal residuals and INP concentration factors measured during CAP-2. These concentration factors represent the enhancement for INP measurements made using an aerosol concentrator compared to ambient concentrations and are dependent on the size of the particles (Section 2.3.1). Measured INP concentration factors during CAP-2 had a maximum value of 37 and a median of 8.3, which are indicated in Figure 5 by the gray shading and gray dashed line, respectively. For reference, the average INP concentration factor measured by Tobo et al. (2013) at a forested site in Colorado was 103, suggesting larger INPs were present than over the SO. Comparison with the aerosol concentrator calibration data implies the INPs measured by

MOORE ET AL. 11 of 20



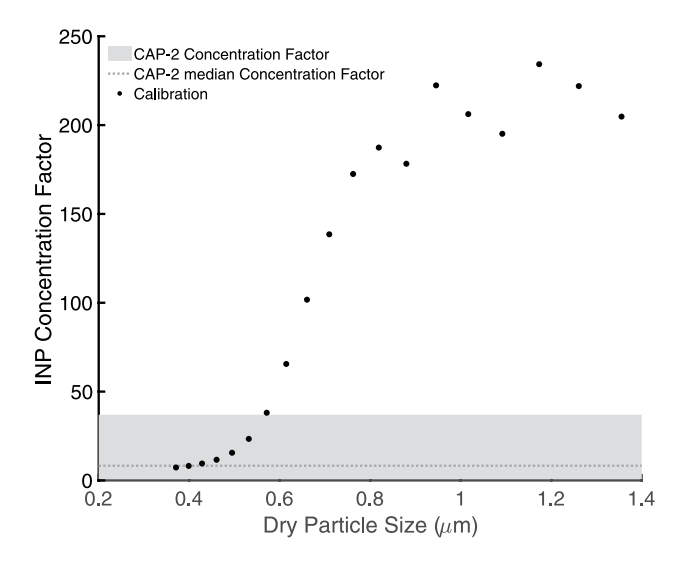


Figure 5. Concentration factor for the aerosol concentrator used during CAP-2 as a function of particle size (black dots). The gray shaded region indicates the range of ice nucleating particle concentration factors measured during CAP-2, and the dashed gray line indicates the project median value.

the CFDC during CAP-2 were dominated by particles <600 nm. CFDC ice crystal residuals collected during CAP-2 and SOC were as small as 0.1 µm; as previously discussed, the maximum size considered was 1.5 µm (Twohy et al., 2021). Ice crystal collections during CAP-2 utilized the aerosol concentrator, so the residual size distribution was corrected for size-dependent enhancements using the calibration data shown in Figure 5, as well as for size-dependent losses in the impactors upstream of the CFDC columns (Section 2.3.1), assuming residuals had the hygroscopicity and density of sea spray aerosols. The corrected median INP residual size was 0.18 µm, which agrees quite well with the 0.3-0.4 µm predicted from the median INP concentration factor measured during CAP-2 (Figure 5), given both have large uncertainties. The smaller than expected sizes of SO INPs, at least during Austral summer, is consistent with the lack of correlation observed by Tatzelt et al. (2022) between ACE INP concentrations and aerosol number or mass, as well as the generally poor or modest relationships found in this study (Section 3.2; Figure 2). Size-resolved INP measurements made in the central Arctic (summer through early fall) by Porter et al. (2022) also noted a surprisingly large contribution of small INPs <0.25 µm in the majority of their samples. By contrast, Creamean et al. (2022) found INPs in the 1-3 µm range dominated in the same region during the summer, and noted the size of INPs shifted over the course of the year-long MOSAiC (Multidisciplinary drifting Observatory for the Study of Climate) campaign. However, compari-

sons with the Arctic should be considered with caution, as previous Arctic studies have indicated a dominance of mineral dust over locally sourced marine INPs (Irish et al., 2019), which is supported by the N_s measurements of Porter et al. (2022) uniformly exceeding the M18 parameterization for marine INPs.

It should be noted that both analyses from CAP-2 and SOC were limited to particles <1.5 μm due to the CFDC upstream impactors necessary to limit interferences from supermicron SSA in optical detection of ice crystals. Another potential complication is the use of measured concentration factors at relatively cold temperatures (≤-25°C) to infer the median size of the overall marine INP population. Mason et al. (2016) found supermicron INPs dominated in most of their continental and coastal sites between -15 and -25°C, and typically measured larger median sizes at warmer temperatures. While biological INPs can be as small as ~10 nm (e.g., Kanji et al., 2017; Pummer et al., 2015; Wilson et al., 2015), many bioaerosols are present in the coarse mode, and typically have warm onset temperatures if active as INPs (e.g., Hoose & Möhler, 2012; Kanji et al., 2017). Although the characteristic size distribution or mode size of ambient marine INPs is unknown, good correlation with aerosol surface area (DeMott et al., 2016; McCluskey et al., 2018c), preferential emission in jet drops over film drops (Wang et al., 2017), and recent laboratory studies indicating supermicron marine INPs dominate below -14°C (Mitts et al., 2021) had suggested the majority of marine INPs are >500 nm, if not larger. However, the excellent agreement between CFDC measurements, which sampled INPs <1.5 µm (CAP-2) or <2.5 µm (SOC), and the IS filter measurements, which captured larger particles, suggest the CFDCs were collecting most available INPs during CAP-2 and SOC (Figures 1 and 7). Future studies of size dependent INP concentrations in remote marine environments are needed to comprehensively assess the size distribution of marine INPs, as well as any seasonality.

3.4. Altitude Dependence

While modeling studies (Burrows et al., 2013; McCluskey et al., 2019, 2023; Vergara-Temprado et al., 2017) have provided insights into the expected vertical distribution of INPs in this region, SOCRATES measurements represent the first in situ observations in and above cloud to validate these results. Although temporally variable, the studies cited predict an increasing influence of mineral dust with height on average. Simulations of the CAPRICORN-1 field campaign (McCluskey et al., 2019) also suggested INP concentrations at -25° C would decrease with height through the boundary layer and up to 3–4 km, then increase at higher altitudes. Some evidence supporting this structure is seen in Figure 6a, which shows the CAP-2 and SOC INP concentrations as a function of altitude. A minimum in mean INP concentrations colder than -27° C was seen between 2 and 4 km, with higher values in the MBL and increasing concentrations at all temperatures between \sim 3 and 6 km. The

MOORE ET AL. 12 of 20

21698996, 2024, 2, Downloaded from https://agupubs.onlinelibrary.wiley.com/doi/10.1029/2023JD039543 by University Of California, Wiley Online Library on [06/02/2024]. See the Terms

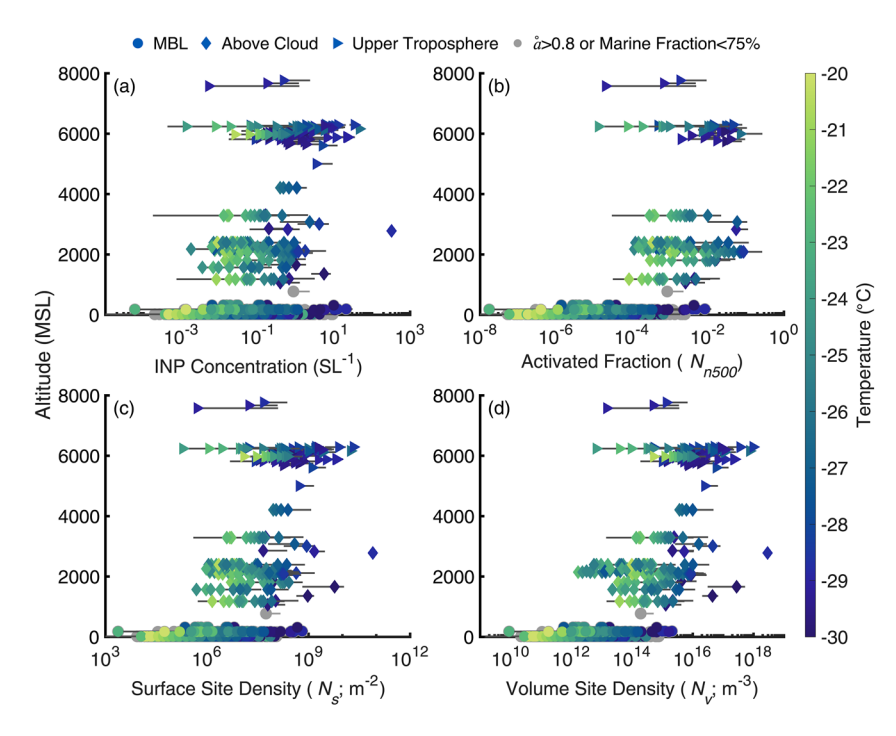


Figure 6. Ice nucleating particle (a) concentration, (b) N_{n500} , (c) N_s and (d) N_v during SOC and CAP-2 as a function of altitude. Data in the marine boundary layer (MBL) are shown as circles, above cloud as diamonds, and upper troposphere (>5,000 m) data as triangles. Non-gray symbols for the MBL data (circles) have $a \le 0.8$ and 5-day back trajectory ocean fraction >75% to isolate marine aerosol; gray symbols do not meet at least one of these criteria. All symbols are colored by measurement temperature.

very limited observations above 6 km did not support the continued increase in INP concentrations with height predicted by McCluskey et al. (2019). The apparent increase in concentration at temperatures warmer than -25° C between the surface and \sim 1 km is likely a result of the higher minimum values observed during SOC than CAP-2 (Section 3.1), and is related to the different sampling strategies, locations, and LOD between the campaigns. When normalized by aerosol concentrations, N_{n500} , N_s and N_v were consistently higher above cloud and in the upper troposphere (>5,000 m) than in the MBL, particularly N_{n500} . This finding is consistent with modeling results predicting different sources of INPs below and above-cloud. It also agrees with TEM measurements of single particles collected during SOCRATES flights, which found significantly increased abundances of crustal and metal particles >0.5 μ m above cloud versus in-cloud or in the MBL (Twohy et al., 2021). Above cloud and upper tropospheric N_{n500} were consistent with the DeMott et al. (2015) parameterization for dust (Figure S6b in Supporting Information S1), but N_s values were still 1–2 orders of magnitude lower than the Ullrich et al. (2017) dust parameterization (Figure S6c in Supporting Information S1). This discrepancy between the effectiveness of dust aerosol number- and surface area-based parameterizations has been reported previously for this region (McCluskey et al., 2019, 2023).

About half of the SOC research flights collected paired filter samples, with one in the MBL and one above cloud. Examples from RF05 (1/25-1/26/18) and RF14 (2/21-2/22/18) are shown in Figure 7, along with SOC CFDC data separated into MBL and above-cloud measurements, in-cloud data on the CVI, and simulated CAM6 INP concentrations (Section 2.4, Text S4 in Supporting Information S1) co-located with the SOC observations (McCluskey et al., 2023). When available, CAP-2 CFDC data during G-V overpasses of the RV *Investigator* are also shown for comparison. Due to the very different speeds traveled by the ship and aircraft, measurements were counted as overpasses if they occurred within 30 min of each other, and the G-V was within 150 km of the RV *Investigator* during the measurement. Within uncertainty, the MBL and above-cloud measurements agreed for both flights shown here (Figures 7a and 7b), as well as the in-cloud observations, which was typical for all of the flights with paired filters. When normalized by n500 (Figures 7c and 7d) or aerosol surface area (Figures 7e and 7f), some separation between the MBL and above-cloud measurements occurred for most flights with available data, with the largest separation for N_{n500} . Both the McCluskey et al. (2018c) clean marine

MOORE ET AL. 13 of 20

21698996, 2024, 2, Downloaded from https://agupubs.onlinelibrary.wiley.com/doi/10.1029/2023JD039543 by University Of California, Wiley Online Library on [06/02/2024]. See the Terms and Conditions (https://onlinelibrary.wiley.com/term

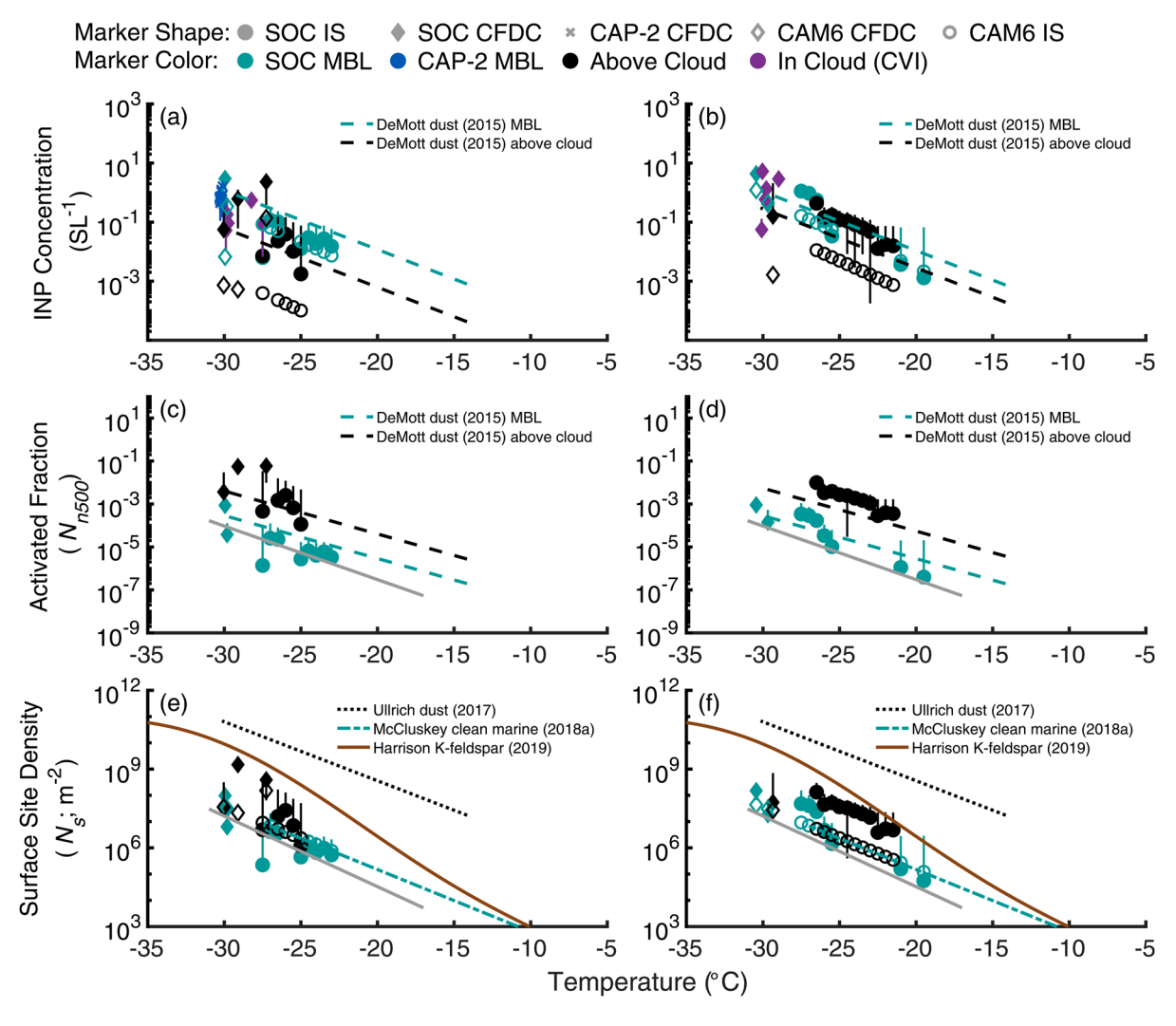


Figure 7. Ice nucleating particle (INP) (a, b) concentration, (c, d) N_{n500} , and (e, f) N_s temperature spectra for SOC flight RF05 (1/25–1/26/18) on the left and RF14 (2/21–2/22/18) on the right. Data in the marine boundary layer (MBL) from SOC are shown as light blue symbols, MBL data from CAP-2 as dark blue symbols, and measurements above cloud in black. SOC filter measurements are circles, SOC Continuous Flow Diffusion Chamber (CFDC) are diamonds, simultaneous CAP-2 CFDC measurements are crosses (if available), and simulated CAM6 INP concentrations are open symbols (panels (a, b) and (e, f) only). If available, SOC CFDC observations in-cloud on the counterflow virtual impactor are shown as purple diamonds in panels (a, b). In panels (a, b) and (c, d), the blue and black dashed lines indicate the DeMott et al. (2015) parameterization for dust based on n500 in the MBL and above cloud, respectively. In (e) and (f), the black dotted line indicates the Ullrich et al. (2017) parameterization for dust N_s , the light blue dot-dash line shows the N_s parameterization from McCluskey et al. (2018c) for clean marine air, and the solid brown line gives the K-feldspar parameterization from Harrison et al. (2019), scaled to 1% as in Harrison et al. (2022). Solid gray lines in (c, d) and (e, f) indicate the best-fit exponential functions to all the MBL data with $a \le 0.8$ and 5-day back trajectory ocean fraction >75% (same as Figure 1).

parameterization and the exponential fit derived in this study predict MBL N_s well on a flight-by-flight basis, while the dust-specific parameterization of Ullrich et al. (2017) uniformly overpredicts N_s , as seen throughout this work. The K-feldspar N_s parameterization from Harrison et al. (2019) is also shown in Figures 7e and 7f, using the 1% scaling factor that was found to work well for African dust in the Caribbean (Harrison et al., 2022). Although an improvement over the Ullrich et al. (2017) parameterization, it still generally overpredicts N_s for both RF05 and RF14. In addition, an appropriate scaling factor for the SO region is unknown, and the INP activity of dust from non-desert regions may not derive from K-feldspar (Testa et al., 2021).

Simulated total INP concentrations from CAM6 have variable agreement with the co-located SOCRATES IS and CFDC measurements. As described in Section 2.4 and Text S4 in Supporting Information S1, CAM6 INP concentrations are the sum of the sea spray INP contribution, based on simulated SSA surface area using M18, and the dust INP contribution, using the number of simulated mineral dust particles larger than 500 nm and the DeMott et al. (2015) parameterization. Overall, the agreement is better for observations in the MBL, while

MOORE ET AL. 14 of 20

simulated above-cloud INP concentrations are biased low, although there is significant variation among flights. The low bias of CAM6 above-cloud values relative to observations is typically reduced when considering N_s (Figures 7e and 7f) instead of INP concentrations (Figures 7a and 7b). This suggests that in addition to the surface level biases in aerosol surface area, low biases in accumulation mode aerosol aloft, and large uncertainties in particle composition aloft observed by McCluskey et al. (2023), there may also be a low bias in simulated aerosol surface area above cloud, which is partially compensating for the underestimation of INPs in CAM6.

Figures 7a–7d include lines indicating the DeMott et al. (2015) INP parameterization for dust. Since D15 is specific to dust INPs but there were not continuous size-resolved measurements of dust concentration, the required dust n500 inputs were estimated using STEM measurements of aerosol composition averaged over SOCRATES (Text S3 in Supporting Information S1; Twohy et al., 2021). The total n500 values measured during each SOC filter collection were scaled using the average fraction of particles >0.5 µm that were categorized as crustal or metal types during SOC (0.5 for above-cloud and 0.02 for MBL) to provide an estimate of dust n500. The dashed blue and black lines in Figures 7a and 7b indicate the dust INP concentrations predicted by D15. Figures 7c and 7d shows D15 normalized by the total n500 measured during each flight, to provide a fair comparison to the SOC INP measurements, and thus represents the predicted N_{n500} if all the INPs present were dust, but SSA contributes to n500. Excellent agreement was seen between both parameterization estimates and their respective filters when normalized by total n500 (Figures 7c and 7d). More variable agreement was seen for absolute INP concentration estimates (Figures 7a and 7b), though most agree with the measurements within uncertainty. In addition to a low bias relative to the SOC observations, CAM6 typically underpredicts INP concentrations relative to D15, especially above cloud (Figures 7a and 7b). Although not explored in McCluskey et al. (2023), this is consistent with the underprediction of dust concentrations observed in E3SMv1 (Raman et al., 2023), as well as an increasing contribution of dust to INP concentrations with height.

While this exercise does not provide direct evidence of the INP types present during SOC, it does support the results shown in Figure 6 and Figure S6 in Supporting Information S1 that different types of INPs dominate at different heights. It also corroborates the results presented in Vergara-Temprado et al. (2017) for global INP simulations, which inferred K-feldspar is an important INP type in the SO during Austral summer, especially at higher altitudes, and intermittently in the MBL. Additionally, if the average amount of dust measured by STEM during SOC was present uniformly across the SO, D15-estimated dust INPs would be sufficient to account for all or nearly all INPs measured, at all heights. This finding emphasizes the vast differences in nucleation efficiency or site density between marine INPs and dust, and shows how even small amounts of long-range transported dust can significantly influence SO cloud properties, as also noted by McCluskey et al. (2023).

4. Summary

The Southern Ocean Cloud Radiation Aerosol Transport Experimental Study (SOCRATES) aircraft campaign, the second Clouds, Aerosols, Precipitation, Radiation and atmospherIc Composition Over the Southern Ocean (CAPRICORN-2) ship campaign, and affiliated projects in 2017–2018 were motivated by a lack of observations and understanding of cloud, aerosol, precipitation, and radiative processes and interactions in the SO region (McFarquhar et al., 2021). This study presents measurements of INPs collected over the SO in austral summer 2018, along with comparisons to CAM6 model simulations. Simultaneous aircraft and ship campaigns provided the first vertical distribution measurements of INPs in the region, including the first in situ observations in and above cloud. Our results confirm recent findings from the ACE (Schmale et al., 2019; Tatzelt et al., 2022; Welti et al., 2020) and CAPRICORN-1 (McCluskey et al., 2018a) campaigns that INP concentrations in the SO MBL are lower at all latitudes than measurements made by Bigg (1973) in the late 1960s and early 1970s. The good agreement between CAP-2 CFDC data and SOC measurements during overpasses (Figure 7) shows promise for future campaigns that might employ a similar multi-platform approach to understand vertical profiles of aerosols and INPs.

Modeling studies (Burrows et al., 2013; McCluskey et al., 2019, 2023; Vergara-Temprado et al., 2017) predicted marine INPs would dominate at low altitudes in the SO, with an increasing influence of mineral dust INPs with height. Paired MBL and above cloud measurements from SOC support this hypothesis (Figure 7). Below- and above-cloud INP concentrations typically agree within uncertainty, however, higher ice nucleation efficiency was found above cloud, consistent with significantly enhanced dust concentrations observed in above-cloud single-particle composition measurements (Twohy et al., 2021). The outsized impact dust INPs can have on SO

MOORE ET AL. 15 of 20

Acknowledgments The authors thank the SOCRATES and CAPRICORN-2 science teams for the excellent planning, operations, and post-campaign discussions, especially PIs Jay Mace, Alain Protat, and Greg McFarquhar. The assistance and support of Cory Wolff and Pavel Romashkin, NCAR project managers for the SOCRATES project, as well as the G-V crew, are greatly appreciated. We especially thank Mike Reeves and Jorgen Jensen of NCAR for calibration, measurements, and analysis of GNI and UHSAS data from SOCRATES. We also thank the CSIRO Marine National Facility (MNF) for its support in the form of sea time on the RV Investigator, support personnel, scientific equipment, and data management during CAPRI-CORN-2. In particular, we wish to thank Ian McRobert (CSIRO Technical Services Officer) for assistance with the RV Investigator's electrical and data management systems during and after CAPRICORN-2, and to Ruhi Humphries (CSIRO Senior Research Scientist), Jason Ward (formerly CSIRO Senior Experimental Scientist) and Melita Keywood (CSIRO Research Director, Earth Systems) for their work maintaining aerosol equipment on board the RV Investigator. We thank Roy Geiss at the Colorado State University Electron Microscopy Lab for performing the STEM analytical measurements. The material in this article is based upon work supported by the National Center for Atmospheric Research, which is a major facility sponsored by the National Science Foundation under Cooperative Agreement 1852977. The data collected during SOCRATES used NSF's Lower Atmosphere Observing Facilities, which are managed and operated by NCAR's Earth Observing Laboratory. The authors gratefully acknowledge the NOAA Air Resources Laboratory (ARL) for the provision of the HYSPLIT transport and dispersion model (https://www.ready. noaa.gov) used in this publication. This work was primarily supported by the National Science Foundation (NSF) through Grant AGS-1660486 (PJD, KAM, TCJH, SMK) and by the United States Department of Energy (DOE) through Grants DE-SC0018929 (PJD. TCJH) and DE-SC0021116 (PJD, TCJH, SMK). KAM acknowledges support by an NSF Graduate Research Fellowship under Grant 006784. CHT was supported by NSF AGS-1660605, DWT and BR by NSF AGS-1660537, and KJS by NSF AGS-1660374. CSM was supported by DOE Grant DE-SC0020098, with travel support from NSF AGS-1660486. This work was partially supported through the NSF Center for Aerosol Impacts on Chemistry of the Environment (CAICE) under Grant CHE-1801971 (KAM, TCJH, PJD). Any opinions, findings, and conclusions or recommendations expressed in this material are those of the author(s)

cloud properties is also demonstrated in Figure 7. Due to the vastly higher nucleation efficiency of mineral dust compared to marine INPs, dust INP concentrations predicted by the D15 parameterization were sufficient to account for almost all INPs measured, both in the MBL and at higher altitudes. However, this was based on bulk aerosol composition measurements and would require the average SOC dust *n500* fraction to be present uniformly over the SO, which global simulations conducted by Vergara-Temprado et al. (2017) suggest is not the case. As a result, the D15 predictions in Figure 7 can only be interpreted as a broad verification of the relatively low nucleation efficiency of marine INPs, which still likely dominate primary ice nucleation in the SO MBL.

Both direct measurements of collected INP residuals and indirect inferences from enhancement factors measured using an aerosol concentrator suggest INPs in the MBL, at least those in the sub-2.5 µm range, are dominated by particles <500 nm during Austral summer. Longer-term measurements and those in other seasons are necessary to understand the seasonality of INP size in this region. Small INP sizes are consistent with the minimal correlations observed between ACE INP concentrations and aerosol number or mass (Tatzelt et al., 2022), as well as the only modest relationships found in this study between INP concentrations and environmental or aerosol metrics (Figure 2). However, both aerosol surface area and wind speed exhibited moderate correlations (p < 0.05) for INP concentrations <-21°C during SOC and CAP-2. Surprisingly, the correlation with wind speed remained after normalizing the INP concentrations by n500, aerosol surface area, or aerosol volume, suggesting marine INP emissions are not strictly proportional to SSA production (Figure 3, Figure S5 in Supporting Information S1). Following the approach of Niemand et al. (2012), a new parameterization for marine INPs was tested, which includes wind speed in addition to activation temperature, and has reduced bias when compared to the existing parameterization of McCluskey et al. (2018). This new parameterization captures the observed mean behavior well, but there is still significant unexplained variability in INP concentrations remaining (Figures 1 and 4). One of the assumptions underlying the Niemand et al. (2012) and M18 approach is that the active site density is constant, or equivalently, the number of INPs per aerosol surface area is fixed. Marine INPs appear to violate this assumption, and wind speed, among other factors, plays a role in how INPs are distributed with aerosol surface area in the remote SO MBL.

Data Availability Statement

All SOCRATES observational data is available from the NCAR/UCAR Earth Observing Laboratory (EOL) repository (https://data.eol.ucar.edu/master_lists/generated/socrates/). This includes navigation, aerosol, and microphysics measurements (UCAR/NCAR—Earth Observing Laboratory, 2019b), VCSEL RH data (UCAR/NCAR—Earth Observing Laboratory, 2020), GNI observations (UCAR/NCAR—Earth Observing Laboratory, 2019a), CFDC data (DeMott et al., 2022), Ice Spectrometer measurements (DeMott & Hill, 2022), and aerosol composition results (Twohy & Toohey, 2020). CAPRICORN-2 CFDC (DeMott & Moore, 2022a), Ice Spectrometer (DeMott & Moore, 2022b), and INP composition (DeMott, 2021) measurements are also available on the SOCRATES EOL repository. SOCRATES CAM6 model simulations are archived online (McCluskey, 2022). All data and samples collected during the CAPRICORN-2 voyage are made publicly available in accordance with CSIRO Marine National Facility policy. Data from the voyage are available at https://doi.org/10.25919/5b71004e37a39 (CSIRO et al., 2018) following registration, and raw data are available by request (data-requests@marine.csiro.au). The time series of predicted exhaust influence on measurements during CAPRICORN-2 is available at https://data.csiro.au/collection/csiro%3A54903v2 (Humphries et al., 2022).

References

Agresti, A., & Coull, B. A. (1998). Approximate is better than "exact" for interval estimation of binomial proportions. *The American Statistician*, 52(2), 119. https://doi.org/10.2307/2685469

Barry, K. R., Hill, T. C. J., Levin, E. J. T., Twohy, C. H., Moore, K. A., Weller, Z. D., et al. (2021). Observations of ice nucleating particles in the free troposphere from western US Wildfires. *Journal of Geophysical Research: Atmospheres*, 126(3), e2020JD033752. https://doi.org/10.1029/2020JD033752

Bassett, G., & Koenker, R. (1978). Asymptotic theory of least absolute error regression. *Journal of the American Statistical Association*, 73(363), 618–622. https://doi.org/10.1080/01621459.1978.10480065

Bigg, E. K. (1973). Ice nucleus concentrations in remote areas. *Journal of the Atmospheric Sciences*, 30(6), 1153–1157. https://doi.org/10.1175/1520-0469(1973)030<1153:INCIRA>2.0.CO;2

Bigg, E. K. (1990). Long-term trends in ice nucleus concentrations. *Atmospheric Research*, 25(5), 409–415. https://doi.org/10.1016/0169-8095(90)90025-8

Bjordal, J., Storelvmo, T., Alterskjær, K., & Carlsen, T. (2020). Equilibrium climate sensitivity above 5°C plausible due to state-dependent cloud feedback. *Nature Geoscience*, 13(11), 718–721. https://doi.org/10.1038/s41561-020-00649-1

MOORE ET AL. 16 of 20

and do not necessarily reflect the views of the National Science Foundation.

- Bodas-Salcedo, A., Hill, P. G., Furtado, K., Williams, K. D., Field, P. R., Manners, J. C., et al. (2016). Large contribution of supercooled liquid clouds to the solar radiation budget of the Southern Ocean. *Journal of Climate*, 29(11), 4213–4228. https://doi.org/10.1175/JCLI-D-15-0564.1
- Bodas-Salcedo, A., Mulcahy, J. P., Andrews, T., Williams, K. D., Ringer, M. A., Field, P. R., & Elsaesser, G. S. (2019). Strong dependence of atmospheric feedbacks on mixed-phase microphysics and aerosol-cloud interactions in HadGEM3. *Journal of Advances in Modeling Earth Systems*, 11(6), 1735–1758. https://doi.org/10.1029/2019MS001688
- Bodas-Salcedo, A., Williams, K. D., Ringer, M. A., Beau, I., Cole, J. N. S., Dufresne, J.-L., et al. (2013). Origins of the solar radiation biases over the Southern Ocean in CFMIP2 models. *Journal of Climate*, 27(1), 41–56. https://doi.org/10.1175/JCLI-D-13-00169.1
- Brockmann, J. E. (2011). Aerosol transport in sampling lines and inlets. In Aerosol measurement (pp. 68–105). John Wiley & Sons, Ltd. https://doi.org/10.1002/9781118001684.ch6
- Bromwich, D. H., Nicolas, J. P., Hines, K. M., Kay, J. E., Key, E. L., Lazzara, M. A., et al. (2012). Tropospheric clouds in Antarctica. Reviews of Geophysics, 50(1), RG1004, https://doi.org/10.1029/2011RG000363
- Burrows, S. M., Hoose, C., Pöschl, U., & Lawrence, M. G. (2013). Ice nuclei in marine air: Biogenic particles or dust? Atmospheric Chemistry and Physics, 13(1), 245–267. https://doi.org/10.5194/acp-13-245-2013
- Chubb, T. H., Jensen, J. B., Siems, S. T., & Manton, M. J. (2013). In situ observations of supercooled liquid clouds over the Southern Ocean during the HIAPER Pole-to-Pole Observation campaigns. Geophysical Research Letters, 40(19), 5280–5285. https://doi.org/10.1002/grl.50986
- Cornwell, G. C., Sultana, C. M., Prank, M., Cochran, R. E., Hill, T. C. J., Schill, G. P., et al. (2020). Ejection of dust from the ocean as a potential source of marine ice nucleating particles. *Journal of Geophysical Research: Atmospheres*, 125(24), e2020JD033073. https://doi.org/10.1029/2020JD033073
- Creamean, J. M., Barry, K., Hill, T. C. J., Hume, C., DeMott, P. J., Shupe, M. D., et al. (2022). Annual cycle observations of aerosols capable of ice formation in central Arctic clouds. *Nature Communications*, 13(1), 3537. https://doi.org/10.1038/s41467-022-31182-x
- CSIRO, Marine National Facility, Rintoul, S. R., Protat, A., Bowie, A. R., Tilbrook, B., & Bodrossy, L. (2018). RV investigator voyage IN2018_ V01 End of Voyage (EOV) archive v4 [Dataset]. CSIRO Data Collection. https://doi.org/10.25919/5b71004e37a39
- DeMott, P. J. (2021). SOCRATES and CAPRICORN-2 single particle INP composition via STEM/EDS (Version 1.0) [Dataset]. UCAR/NCAR—Earth Observing Laboratory. https://doi.org/10.26023/THHB-X79P-A006
- DeMott, P. J., Hill, T. C., Marchand, R., & Alexander, S. (2018). Macquarie Island Cloud and Radiation Experiment (MICRE) ice nucleating particle measurements field campaign report (No. DOE/SC-ARM-18-030). ARM User Facility, Pacific Northwest National Laboratory. Retrieved from https://www.osti.gov/biblio/1489359
- DeMott, P. J., Hill, T. C., & McFarquhar, G. (2018). Measurements of Aerosols, Radiation, and Clouds over the Southern Ocean (MARCUS) ice nucleating particle measurements field campaign report (No. DOE/SC-ARM-18-031). ARM User Facility, Pacific Northwest National Laboratory. Retrieved from https://www.osti.gov/biblio/1489372
- DeMott, P. J., & Hill, T. C. J. (2022). NSF/NCAR GV HIAPER ice spectrometer data [Dataset]. UCAR/NCAR—Earth Observing Laboratory. https://doi.org/10.26023/TTHZ-474E-B211
- DeMott, P. J., Hill, T. C. J., McCluskey, C. S., Prather, K. A., Collins, D. B., Sullivan, R. C., et al. (2016). Sea spray aerosol as a unique source of ice nucleating particles. *Proceedings of the National Academy of Sciences*, 113(21), 5797–5803. https://doi.org/10.1073/pnas.1514034112
- DeMott, P. J., Möhler, O., Cziczo, D. J., Hiranuma, N., Petters, M. D., Petters, S. S., et al. (2018). The Fifth International Workshop on Ice Nucleation phase 2 (FIN-02): Laboratory intercomparison of ice nucleation measurements. Atmospheric Measurement Techniques, 11(11), 6231–6257. https://doi.org/10.5194/amt-11-6231-2018
- DeMott, P. J., & Moore, K. A. (2022a). CAPRICORN R/V investigator continuous flow diffusion chamber measurements [Dataset]. UCAR/NCAR—Earth Observing Laboratory. https://doi.org/10.26023/K5NQ-P9AB-KH06
- DeMott, P. J., & Moore, K. A. (2022b). CAPRICORN R/V investigator ice spectrometer measurements [Dataset]. UCAR/NCAR—Earth Observing Laboratory. https://doi.org/10.26023/RTYY-YDBS-6W06
- DeMott, P. J., Moore, K. A., & McCluskey, C. S. (2022). SOCRATES: NSF/NCAR GV HIAPER continuous flow diffusion chamber measurements [Dataset]. UCAR/NCAR—Earth Observing Laboratory. https://doi.org/10.26023/P469-803K-WP0W
- DeMott, P. J., Prenni, A. J., Liu, X., Kreidenweis, S. M., Petters, M. D., Twohy, C. H., et al. (2010). Predicting global atmospheric ice nuclei distributions and their impacts on climate. *Proceedings of the National Academy of Sciences*, 107(25), 11217–11222. https://doi.org/10.1073/pnas.0010818107
- DeMott, P. J., Prenni, A. J., McMeeking, G. R., Sullivan, R. C., Petters, M. D., Tobo, Y., et al. (2015). Integrating laboratory and field data to quantify the immersion freezing ice nucleation activity of mineral dust particles. Atmospheric Chemistry and Physics, 15(1), 393–409. https:// doi.org/10.5194/acp-15-393-2015
- Frey, W. R., & Kay, J. E. (2017). The influence of extratropical cloud phase and amount feedbacks on climate sensitivity. *Climate Dynamics*, 50(7), 3097–3116. https://doi.org/10.1007/s00382-017-3796-5
- Gantt, B., Meskhidze, N., Facchini, M. C., Rinaldi, M., Ceburnis, D., & O'Dowd, C. D. (2011). Wind speed dependent size-resolved parameterization for the organic mass fraction of sea spray aerosol. Atmospheric Chemistry and Physics, 11(16), 8777–8790. https://doi.org/10.5194/ acp-11-8777-2011
- Gettelman, A., Bardeen, C. G., McCluskey, C. S., Järvinen, E., Stith, J., Bretherton, C., et al. (2020). Simulating observations of Southern Ocean clouds and implications for climate. *Journal of Geophysical Research: Atmospheres*, 125(21), e2020JD032619. https://doi.org/10.1029/2020JD032619
- Ginoux, P., Prospero, J. M., Gill, T. E., Hsu, N. C., & Zhao, M. (2012). Global-scale attribution of anthropogenic and natural dust sources and their emission rates based on MODIS Deep Blue aerosol products. Reviews of Geophysics, 50(3), RG3005. https://doi.org/10.1029/2012RG000388
- Harrison, A. D., Lever, K., Sanchez-Marroquin, A., Holden, M. A., Whale, T. F., Tarn, M. D., et al. (2019). The ice-nucleating ability of quartz immersed in water and its atmospheric importance compared to K-feldspar. *Atmospheric Chemistry and Physics*, 19(17), 11343–11361. https://doi.org/10.5194/acp-19-11343-2019
- Harrison, A. D., O'Sullivan, D., Adams, M. P., Porter, G. C. E., Blades, E., Brathwaite, C., et al. (2022). The ice-nucleating activity of African mineral dust in the Caribbean boundary layer. Atmospheric Chemistry and Physics, 22(14), 9663–9680. https://doi.org/10.5194/acp-22-9663-2022
- Hiranuma, N., Augustin-Bauditz, S., Bingemer, H., Budke, C., Curtius, J., Danielczok, A., et al. (2015). A comprehensive laboratory study on the immersion freezing behavior of illite NX particles: A comparison of 17 ice nucleation measurement techniques. Atmospheric Chemistry and Physics, 15(5), 2489–2518. https://doi.org/10.5194/acp-15-2489-2015
- Hoose, C., & Möhler, O. (2012). Heterogeneous ice nucleation on atmospheric aerosols: A review of results from laboratory experiments. Atmospheric Chemistry and Physics, 12(20), 9817–9854. https://doi.org/10.5194/acp-12-9817-2012
- Humphries, R. S., Keywood, M. D., Gribben, S., McRobert, I. M., Ward, J. P., Selleck, P., et al. (2021). Southern Ocean latitudinal gradients of cloud condensation nuclei. Atmospheric Chemistry and Physics, 21(16), 12757–12782. https://doi.org/10.5194/acp-21-12757-2021

MOORE ET AL. 17 of 20

- Humphries, R. S., McRobert, I. M., Ponsonby, W. A., Ward, J. P., Keywood, M. D., Loh, Z. M., et al. (2022). Exhaust identification data from IN2018_V01 (CAPRICORN2) [Dataset]. https://doi.org/10.25919/f8s8-cy20
- Irish, V. E., Hanna, S. J., Willis, M. D., China, S., Thomas, J. L., Wentzell, J. J. B., et al. (2019). Ice nucleating particles in the marine boundary layer in the Canadian Arctic during summer 2014. *Atmospheric Chemistry and Physics*, 19(2), 1027–1039. https://doi.org/10.5194/acp-19-1027-2019
- Järvinen, E., McCluskey, C. S., Waitz, F., Schnaiter, M., Bansemer, A., Bardeen, C. G., et al. (2022). Evidence for secondary ice production in Southern Ocean maritime boundary layer clouds. *Journal of Geophysical Research: Atmospheres*, 127(16), e2021JD036411. https://doi. org/10.1029/2021JD036411
- Kanji, Z. A., Ladino, L. A., Wex, H., Boose, Y., Burkert-Kohn, M., Cziczo, D. J., & Krämer, M. (2017). Overview of ice nucleating particles. Meteorological Monographs, 58, 1.1–1.33. https://doi.org/10.1175/AMSMONOGRAPHS-D-16-0006.1
- Kay, J. E., Bourdages, L., Miller, N. B., Morrison, A., Yettella, V., Chepfer, H., & Eaton, B. (2016a). Evaluating and improving cloud phase in the Community Atmosphere Model version 5 using spaceborne lidar observations. *Journal of Geophysical Research: Atmospheres*, 121(8), 4162–4176. https://doi.org/10.1002/2015JD024699
- Kay, J. E., Wall, C., Yettella, V., Medeiros, B., Hannay, C., Caldwell, P., & Bitz, C. (2016b). Global climate impacts of fixing the Southern Ocean shortwave radiation bias in the Community Earth System Model (CESM). *Journal of Climate*, 29(12), 4617–4636. https://doi.org/10.1175/ ICLI-D-15-0358.1
- Kremser, S., Harvey, M., Kuma, P., Hartery, S., Saint-Macary, A., McGregor, J., et al. (2021). Southern Ocean cloud and aerosol data: A compilation of measurements from the 2018 Southern Ocean Ross Sea Marine Ecosystems and Environment voyage. *Earth System Science Data*, 13(7), 3115–3153. https://doi.org/10.5194/essd-13-3115-2021
- Krishnamoorthy, K., & Lee, M. (2012). New approximate confidence intervals for the difference between two Poisson means and comparison. Journal of Statistical Computation and Simulation, 83(12), 2232–2243. https://doi.org/10.1080/00949655.2012.686616
- Li, G., Wieder, J., Pasquier, J. T., Henneberger, J., & Kanji, Z. A. (2022). Predicting atmospheric background number concentration of ice-nucleating particles in the Arctic. *Atmospheric Chemistry and Physics*, 22(21), 14441–14454. https://doi.org/10.5194/acp-22-14441-2022
- Mace, G. G., Protat, A., Humphries, R. S., Alexander, S. P., McRobert, I. M., Ward, J., et al. (2020). Southern Ocean cloud properties derived from CAPRICORN and MARCUS Data. *Journal of Geophysical Research: Atmospheres*, 126(4), e2020JD033368. https://doi. org/10.1029/2020JD033368
- Maring, H., Savoie, D. L., Izaguirre, M. A., Custals, L., & Reid, J. S. (2003). Mineral dust aerosol size distribution change during atmospheric transport. *Journal of Geophysical Research*, 108(D19), 8592. https://doi.org/10.1029/2002JD002536
- Mason, R. H., Si, M., Chou, C., Irish, V. E., Dickie, R., Elizondo, P., et al. (2016). Size-resolved measurements of ice-nucleating particles at six locations in North America and one in Europe. Atmospheric Chemistry and Physics, 16(3), 1637–1651. https://doi.org/10.5194/acp-16-1637-2016
- McCluskey, C. S. (2022). Archived model output for "Simulating observations of Southern Ocean clouds and implications for climate" (Version 1) [Dataset]. Zenodo. https://doi.org/10.5281/zenodo.6463951
- McCluskey, C. S., DeMott, P. J., Ma, P.-L., & Burrows, S. M. (2019). Numerical representations of marine ice-nucleating particles in remote marine environments evaluated against observations. *Geophysical Research Letters*, 46(13), 7838–7847. https://doi.org/10.1029/2018GL081861
- McCluskey, C. S., DeMott, P. J., Prenni, A. J., Levin, E. J. T., McMeeking, G. R., Sullivan, A. P., et al. (2014). Characteristics of atmospheric ice nucleating particles associated with biomass burning in the US: Prescribed burns and wildfires. *Journal of Geophysical Research: Atmospheres*, 119(17), 10458–10470. https://doi.org/10.1002/2014JD021980
- McCluskey, C. S., Gettelman, A., Bardeen, C. G., DeMott, P. J., Moore, K. A., Kreidenweis, S. M., et al. (2023). Simulating Southern Ocean aerosol and ice nucleating particles in the Community Earth System Model Version 2. *Journal of Geophysical Research: Atmospheres*, n/a(n/a), e2022JD036955. https://doi.org/10.1029/2022JD036955
- McCluskey, C. S., Hill, T. C. J., Humphries, R. S., Rauker, A. M., Moreau, S., Strutton, P. G., et al. (2018a). Observations of ice nucleating particles over Southern Ocean waters. Geophysical Research Letters, 45(21), 11989–11997. https://doi.org/10.1029/2018GL079981
- McCluskey, C. S., Hill, T. C. J., Sultana, C. M., Laskina, O., Trueblood, J., Santander, M. V., et al. (2018b). A mesocosm double feature: Insights into the chemical makeup of marine ice nucleating particles. *Journal of the Atmospheric Sciences*, 75(7), 2405–2423. https://doi.org/10.1175/
- McCluskey, C. S., Ovadnevaite, J., Rinaldi, M., Atkinson, J., Belosi, F., Ceburnis, D., et al. (2018c). Marine and terrestrial organic ice-nucleating particles in pristine marine to continentally influenced Northeast Atlantic air masses. *Journal of Geophysical Research: Atmospheres*, 123(11), 6196–6212. https://doi.org/10.1029/2017JD028033
- McFarquhar, G. M., Bretherton, C. S., Marchand, R., Protat, A., DeMott, P. J., Alexander, S. P., et al. (2021). Observations of clouds, aerosols, precipitation, and surface radiation over the Southern Ocean: An overview of CAPRICORN, MARCUS, MICRE, and SOCRATES. *Bulletin of the American Meteorological Society*, 102(4), E894–E928. https://doi.org/10.1175/BAMS-D-20-0132.1
- Mitts, B. A., Wang, X., Lucero, D. D., Beall, C. M., Deane, G. B., DeMott, P. J., & Prather, K. A. (2021). Importance of supermicron ice nucleating particles in nascent sea spray. Geophysical Research Letters, 48(3), e2020GL089633. https://doi.org/10.1029/2020GL089633
- Miyakawa, T., Taketani, F., Tobo, Y., Matsumoto, K., Yoshizue, M., Takigawa, M., & Kanaya, Y. (2023). Measurements of aerosol particle size distributions and INPs over the Southern Ocean in the late austral summer of 2017 on Board the R/V Mirai: Importance of the marine boundary layer structure. *Earth and Space Science*, 10(3), e2022EA002736. https://doi.org/10.1029/2022EA002736
- Monahan, E. C., Spiel, D. E., & Davidson, K. L. (1986). A model of marine aerosol generation via whitecaps and wave disruption. In E. C. Monahan & G. M. Niocaill (Eds.), *Oceanic whitecaps: And their role in air-sea exchange processes* (pp. 167–174). Springer Netherlands. https://doi.org/10.1007/978-94-009-4668-2_16
- Moore, K. A. (2020). Constraining marine ice nucleating particle parameterizations in atmospheric models using observations from the Southern Ocean (MS Thesis). Colorado State University. Retrieved from https://mountainscholar.org/handle/10217/208435
- Moore, K. A., Alexander, S. P., Humphries, R. S., Jensen, J., Protat, A., Reeves, J. M., et al. (2022). Estimation of sea spray aerosol surface area over the Southern Ocean using scattering measurements. *Journal of Geophysical Research: Atmospheres*, 127(22), e2022JD037009. https://doi.org/10.1029/2022JD037009
- Morrison, A. E., Siems, S. T., & Manton, M. J. (2011). A three-year climatology of cloud-top phase over the Southern Ocean and North Pacific. Journal of Climate, 24(9), 2405–2418. https://doi.org/10.1175/2010JCL13842.1
- Naud, C. M., Booth, J. F., & Genio, A. D. D. (2014). Evaluation of ERA-interim and MERRA cloudiness in the Southern Ocean. *Journal of Climate*, 27(5), 2109–2124. https://doi.org/10.1175/JCLI-D-13-00432.1
- Niemand, M., Möhler, O., Vogel, B., Vogel, H., Hoose, C., Connolly, P., et al. (2012). A particle-surface-area-based parameterization of immersion freezing on desert dust particles. *Journal of the Atmospheric Sciences*, 69(10), 3077–3092. https://doi.org/10.1175/JAS-D-11-0249.1

MOORE ET AL. 18 of 20

- Noone, K. J., Ogren, J. A., Heintzenberg, J., Charlson, R. J., & Covert, D. S. (1988). Design and calibration of a counterflow virtual impactor for sampling of atmospheric fog and cloud droplets. *Aerosol Science and Technology*, 8(3), 235–244. https://doi.org/10.1080/02786828808959186
- O'Dowd, C. D., & de Leeuw, G. (2007). Marine aerosol production: A review of the current knowledge. *Philosophical Transactions of the Royal Society A: Mathematical, Physical and Engineering Sciences*, 365(1856), 1753–1774. https://doi.org/10.1098/rsta.2007.2043
- O'Sullivan, D., Murray, B. J., Ross, J. F., Whale, T. F., Price, H. C., Atkinson, J. D., et al. (2015). The relevance of nanoscale biological fragments for ice nucleation in clouds. *Scientific Reports*, 5(1), 8082. https://doi.org/10.1038/srep08082
- Porter, G. C. E., Adams, M. P., Brooks, I. M., Ickes, L., Karlsson, L., Leck, C., et al. (2022). Highly active ice-nucleating particles at the summer north pole. *Journal of Geophysical Research: Atmospheres*, 127(6), e2021JD036059. https://doi.org/10.1029/2021JD036059
- Pruppacher, H. R., & Klett, J. D. (2010). Microphysics of clouds and precipitation (2nd ed.). Springer Netherlands. https://doi. org/10.1007/978-0-306-48100-0
- Pummer, B. G., Budke, C., Augustin-Bauditz, S., Niedermeier, D., Felgitsch, L., Kampf, C. J., et al. (2015). Ice nucleation by water-soluble macromolecules. Atmospheric Chemistry and Physics, 15(8), 4077–4091. https://doi.org/10.5194/acp-15-4077-2015
- Quinn, P. K., Coffman, D. J., Johnson, J. E., Upchurch, L. M., & Bates, T. S. (2017). Small fraction of marine cloud condensation nuclei made up of sea spray aerosol. *Nature Geoscience*, 10(9), 674–679. https://doi.org/10.1038/ngeo3003
- Raman, A., Hill, T., DeMott, P. J., Singh, B., Zhang, K., Ma, P.-L., et al. (2023). Long-term variability in immersion-mode marine ice-nucleating particles from climate model simulations and observations. *Atmospheric Chemistry and Physics*, 23(10), 5735–5762. https://doi.org/10.5194/acn-23-5735-2023
- Rogers, D. C. (1988). Development of a continuous flow thermal gradient diffusion chamber for ice nucleation studies. Atmospheric Research, 22(2), 149–181. https://doi.org/10.1016/0169-8095(88)90005-1
- Rogers, D. C., DeMott, P. J., Kreidenweis, S. M., & Chen, Y. (2001). A continuous-flow diffusion chamber for airborne measurements of ice nuclei. *Journal of Atmospheric and Oceanic Technology*, 18(5), 17–741. https://doi.org/10.1175/1520-0426(2001)018<0725:acfdcf>2.0.co;2
- Rolph, G., Stein, A., & Stunder, B. (2017). Real-time Environmental Applications and Display sYstem: READY. Environmental Modelling & Software, 95, 210–228. https://doi.org/10.1016/j.envsoft.2017.06.025
- Rosenfeld, D., Chemke, R., DeMott, P. J., Sullivan, R. C., Rasmussen, R., McDonough, F., et al. (2013). The common occurrence of highly supercooled drizzle and rain near the coastal regions of the western United States. *Journal of Geophysical Research: Atmospheres*, 118(17), 9819–9833. https://doi.org/10.1002/jgrd.50529
- Rosinski, J., Haagenson, P. L., Nagamoto, C. T., & Parungo, F. (1987). Nature of ice-forming nuclei in marine air masses. *Journal of Aerosol Science*, 18(3), 291–309. https://doi.org/10.1016/0021-8502(87)90024-3
- Sanchez, K. J., Zhang, B., Liu, H., Saliba, G., Chen, C.-L., Lewis, S. L., et al. (2021). Linking marine phytoplankton emissions, meteorological processes, and downwind particle properties with FLEXPART. Atmospheric Chemistry and Physics, 21(2), 831–851. https://doi.org/10.5194/acp-21-831-2021
- Schill, G. P., Jathar, S. H., Kodros, J. K., Levin, E. J. T., Galang, A. M., Friedman, B., et al. (2016). Ice-nucleating particle emissions from photochemically aged diesel and biodiesel exhaust. *Geophysical Research Letters*, 43(10), 5524–5531. https://doi.org/10.1002/2016GL069529
- Schmale, J., Baccarini, A., Thurnherr, I., Henning, S., Efraim, A., Regayre, L., et al. (2019). Overview of the Antarctic Circumnavigation Expedition: Study of Preindustrial-like Aerosols and their Climate Effects (ACE-SPACE). *Bulletin of the American Meteorological Society*, 100(11), 2260–2283. https://doi.org/10.1175/BAMS-D-18-0187.1
- Sofiev, M., Soares, J., Prank, M., de Leeuw, G., & Kukkonen, J. (2011). A regional-to-global model of emission and transport of sea salt particles in the atmosphere. *Journal of Geophysical Research*, 116(D21), D21302. https://doi.org/10.1029/2010JD014713
- Stein, A. F., Draxler, R. R., Rolph, G. D., Stunder, B. J. B., Cohen, M. D., & Ngan, F. (2015). NOAA's HYSPLIT atmospheric transport and dispersion modeling system. *Bulletin of the American Meteorological Society*, 96(12), 2059–2077. https://doi.org/10.1175/BAMS-D-14-00110.1
- Stith, J. L., Ramanathan, V., Cooper, W. A., Roberts, G. C., DeMott, P. J., Carmichael, G., et al. (2009). An overview of aircraft observations from the Pacific Dust Experiment campaign. *Journal of Geophysical Research*, 114(D5), D05207. https://doi.org/10.1029/2008JD010924
- Tan, I., Storelvmo, T., & Zelinka, M. D. (2016). Observational constraints on mixed-phase clouds imply higher climate sensitivity. Science, 352(6282), 224–227. https://doi.org/10.1126/science.aad5300
- Tatzelt, C., Henning, S., Welti, A., Baccarini, A., Hartmann, M., Gysel-Beer, M., et al. (2022). Circum-Antarctic abundance and properties of CCN and INPs. Atmospheric Chemistry and Physics, 22(14), 9721–9745. https://doi.org/10.5194/acp-22-9721-2022
- Testa, B., Hill, T. C. J., Marsden, N. A., Barry, K. R., Hume, C. C., Bian, Q., et al. (2021). Ice nucleating particle connections to regional Argentinian land surface emissions and weather during the cloud, aerosol, and complex terrain interactions experiment. *Journal of Geophysical Research: Atmospheres*, 126(23), e2021JD035186. https://doi.org/10.1029/2021JD035186
- Tobo, Y., Prenni, A. J., DeMott, P. J., Huffman, J. A., McCluskey, C. S., Tian, G., et al. (2013). Biological aerosol particles as a key determinant of ice nuclei populations in a forest ecosystem. *Journal of Geophysical Research: Atmospheres*, 118(17), 10100–10110. https://doi.org/10.1002/igrd.50801
- Twohy, C. H., DeMott, P. J., Pratt, K. A., Subramanian, R., Kok, G. L., Murphy, S. M., et al. (2010). Relationships of biomass-burning aerosols to ice in orographic wave clouds. *Journal of the Atmospheric Sciences*, 67(8), 2437–2450. https://doi.org/10.1175/2010JAS3310.1
- Twohy, C. H., DeMott, P. J., Russell, L. M., Toohey, D. W., Rainwater, B., Geiss, R., et al. (2021). Cloud-nucleating particles over the southern ocean in a changing climate. *Earth's Future*, 9(3), e2020EF001673. https://doi.org/10.1029/2020EF001673
- Twohy, C. H., McMeeking, G. R., DeMott, P. J., McCluskey, C. S., Hill, T. C. J., Burrows, S. M., et al. (2016). Abundance of fluorescent biological aerosol particles at temperatures conducive to the formation of mixed-phase and cirrus clouds. *Atmospheric Chemistry and Physics*, 16(13), 8205–8225. https://doi.org/10.5194/acp-16-8205-2016
- Twohy, C. H., & Toohey, D. W. (2020). Single particle composition via STEM/EDS (Version 1.0) [Dataset]. UCAR/NCAR—Earth Observing Laboratory. https://doi.org/10.26023/55HP-PSEF-WC07
- UCAR/NCAR—Earth Observing Laboratory. (2005). NSF/NCAR GV HIAPER aircraft. UCAR/NCAR—Earth Observing Laboratory. https://doi.org/10.5065/D6DR2SJP
- UCAR/NCAR—Earth Observing Laboratory. (2019a). SOCRATES: Giant Cloud Condensation Nuclei (CCN) impactor data [Dataset]. UCAR/NCAR—Earth Observing Laboratory. Retrieved from https://data.eol.ucar.edu/dataset/552.048
- UCAR/NCAR—Earth Observing Laboratory. (2019b). UCAR/NCAR Earth Observing Laboratory: Low Rate (LRT -1 sps) navigation, state parameter, and microphysics flight-level data Version 1.3 [Dataset]. UCAR/NCAR—Earth Observing Laboratory. https://doi.org/10.5065/D6M32TM9
- UCAR/NCAR—Earth Observing Laboratory. (2020). UCAR/NCAR Earth Observing Laboratory: VCSEL 1Hz water vapor data Version 1.0 [Dataset]. UCAR/NCAR—Earth Observing Laboratory. https://doi.org/10.26023/KFSD-Y8DQ-YC0D
- Ullrich, R., Hoose, C., Möhler, O., Niemand, M., Wagner, R., Höhler, K., et al. (2017). A new ice nucleation active site parameterization for desert dust and soot. *Journal of the Atmospheric Sciences*, 74(3), 699–717. https://doi.org/10.1175/JAS-D-16-0074.1

MOORE ET AL. 19 of 20

- Vali, G. (1971). Quantitative evaluation of experimental results on the heterogeneous freezing nucleation of supercooled liquids. *Journal of the Atmospheric Sciences*, 28(3), 402–409. https://doi.org/10.1175/1520-0469(1971)028<0402:QEOERA>2.0.CO;2
- Vergara-Temprado, J., Miltenberger, A. K., Furtado, K., Grosvenor, D. P., Shipway, B. J., Hill, A. A., et al. (2018). Strong control of Southern Ocean cloud reflectivity by ice-nucleating particles. *Proceedings of the National Academy of Sciences*, 115(11), 2687–2692. https://doi.org/10.1073/pnas.1721627115
- Vergara-Temprado, J., Murray, B. J., Wilson, T. W., O'Sullivan, D., Browse, J., Pringle, K. J., et al. (2017). Contribution of feldspar and marine organic aerosols to global ice nucleating particle concentrations. *Atmospheric Chemistry and Physics*, 17(5), 3637–3658. https://doi.org/10.5194/acp-17-3637-2017
- von der Weiden, S.-L., Drewnick, F., & Borrmann, S. (2009). Particle Loss Calculator A new software tool for the assessment of the performance of aerosol inlet systems. Atmospheric Measurement Techniques, 2(2), 479–494. https://doi.org/10.5194/amt-2-479-2009
- Wang, X., Deane, G. B., Moore, K. A., Ryder, O. S., Stokes, M. D., Beall, C. M., et al. (2017). The role of jet and film drops in controlling the mixing state of submicron sea spray aerosol particles. *Proceedings of the National Academy of Sciences*, 114(27), 6978–6983. https://doi. org/10.1073/pnas.1702420114
- Welti, A., Bigg, E. K., DeMott, P. J., Gong, X., Hartmann, M., Harvey, M., et al. (2020). Ship-based measurements of ice nuclei concentrations over the Arctic, Atlantic, Pacific and Southern oceans. Atmospheric Chemistry and Physics, 20(23), 15191–15206. https://doi.org/10.5194/ acp-20-15191-2020
- Wilson, T. W., Ladino, L. A., Alpert, P. A., Breckels, M. N., Brooks, I. M., Browse, J., et al. (2015). A marine biogenic source of atmospheric ice-nucleating particles. *Nature*, 525(7568), 234–238. https://doi.org/10.1038/nature14986
- Zelinka, M. D., Myers, T. A., McCoy, D. T., Po-Chedley, S., Caldwell, P. M., Ceppi, P., et al. (2020). Causes of higher climate sensitivity in CMIP6 models. Geophysical Research Letters, 47(1), e2019GL085782. https://doi.org/10.1029/2019GL085782
- Zhao, X., Liu, X., Burrows, S., DeMott, P. J., Diao, M., McFarquhar, G. M., et al. (2023). Important ice processes are missed by the community earth system model in Southern Ocean mixed-phase clouds: Bridging SOCRATES observations to model developments. *Journal of Geophysical Research: Atmospheres*, 128(4), e2022JD037513. https://doi.org/10.1029/2022JD037513

References From the Supporting Information

- Clegg, S. L., Brimblecombe, P., & Wexler, A. S. (1998). Thermodynamic model of the system H⁺-NH₄⁺-Na⁺-SO₄²⁻-NO₃⁻-Cl⁻-H₂O at 298.15 K. The Journal of Physical Chemistry A, 102(12), 2155–2171. https://doi.org/10.1021/jp973043j
- Clegg, S. L., Brimblecombe, P., & Wexler, A. S. (2021). E-AIM home page. Retrieved from http://www.aim.env.uea.ac.uk/aim/aim.php
- Gettelman, A., Mills, M. J., Kinnison, D. E., Garcia, R. R., Smith, A. K., Marsh, D. R., et al. (2019). The Whole Atmosphere Community Climate Model Version 6 (WACCM6). *Journal of Geophysical Research: Atmospheres*, 124(23), 12380–12403. https://doi.org/10.1029/2019JD030943 Humphries, R. S., McRobert, I. M., Ponsonby, W. A., Ward, J. P., Keywood, M. D., Loh, Z. M., et al. (2019). Identification of platform exhaust on
- the RV Investigator. Atmospheric Measurement Techniques, 12(6), 3019–3038. https://doi.org/10.5194/amt-12-3019-2019
 Jensen, J. B., Beaton, S. P., Stith, J. L., Schwenz, K., Colón-Robles, M., Rauber, R. M., & Gras, J. (2020). The Giant Nucleus Impactor (GNI)—A
- system for the impaction and automated optical sizing of giant aerosol particles with emphasis on sea salt. Part I: Basic instrument and algorithms. *Journal of Atmospheric and Oceanic Technology*, 37(9), 1551–1569. https://doi.org/10.1175/JTECH-D-19-0109.1

 Lance, S., Brock, C. A., Rogers, D., & Gordon, J. A. (2010). Water droplet calibration of the Cloud Droplet Probe (CDP) and in-flight performance
- in liquid, ice and mixed-phase clouds during ARCPAC. Atmospheric Measurement Techniques, 3(6), 1683–1706. https://doi.org/10.5194/amt-3-1683-2010
- Liu, X., Ma, P.-L., Wang, H., Tilmes, S., Singh, B., Easter, R. C., et al. (2016). Description and evaluation of a new four-mode version of the Modal Aerosol Module (MAM4) within version 5.3 of the Community Atmosphere Model. *Geoscientific Model Development*, 9(2), 505–522. https://doi.org/10.5194/gmd-9-505-2016
- Mårtensson, E. M., Nilsson, E. D., de Leeuw, G., Cohen, L. H., & Hansson, H.-C. (2003). Laboratory simulations and parameterization of the primary marine aerosol production. *Journal of Geophysical Research*, 108(D9), 4297. https://doi.org/10.1029/2002JD002263
- Modini, R. L., Frossard, A. A., Ahlm, L., Russell, L. M., Corrigan, C. E., Roberts, G. C., et al. (2015). Primary marine aerosol-cloud interactions off the coast of California. *Journal of Geophysical Research: Atmospheres*, 120(9), 4282–4303. https://doi.org/10.1002/2014JD022963
- Monahan, E. C., & Muircheartaigh, I. (1980). Optimal power-law description of oceanic whitecap coverage dependence on wind speed. *Journal of Physical Oceanography*, 10(12), 2094–2099. https://doi.org/10.1175/1520-0485(1980)010<2094:OPLDOO>2.0.CO;2
- Sanchez, K. J., Roberts, G. C., Saliba, G., Russell, L. M., Twohy, C., Reeves, J. M., et al. (2021). Measurement report: Cloud processes and the transport of biological emissions affect Southern Ocean particle and cloud condensation nuclei concentrations. Atmospheric Chemistry and Physics, 21(5), 3427–3446. https://doi.org/10.5194/acp-21-3427-2021
- Tang, I. N., Tridico, A. C., & Fung, K. H. (1997). Thermodynamic and optical properties of sea salt aerosols. *Journal of Geophysical Research*, 102(D19), 23269–23275. https://doi.org/10.1029/97JD01806
- Zender, C. S., Bian, H., & Newman, D. (2003). Mineral Dust Entrainment and Deposition (DEAD) model: Description and 1990s dust climatology. *Journal of Geophysical Research*, 108(D14), 4416. https://doi.org/10.1029/2002JD002775

MOORE ET AL. 20 of 20